AD-A105 003 GTE LABS INC WALTHAM MA F/G 20/3
FUNDAMENTALS OF MAGNETIC INTERACTIONS: NEW APPROACHES TO THEORY--ETC(U)
AUG 81 A LEMPICKI, W J MINISCALCO F49620-79-C-0182
UNCLASSIFIED AFOSR-TR-81-0676 NL

1 OF 1
AD
A105003

END
DATE FILMED
10-81
DTIC

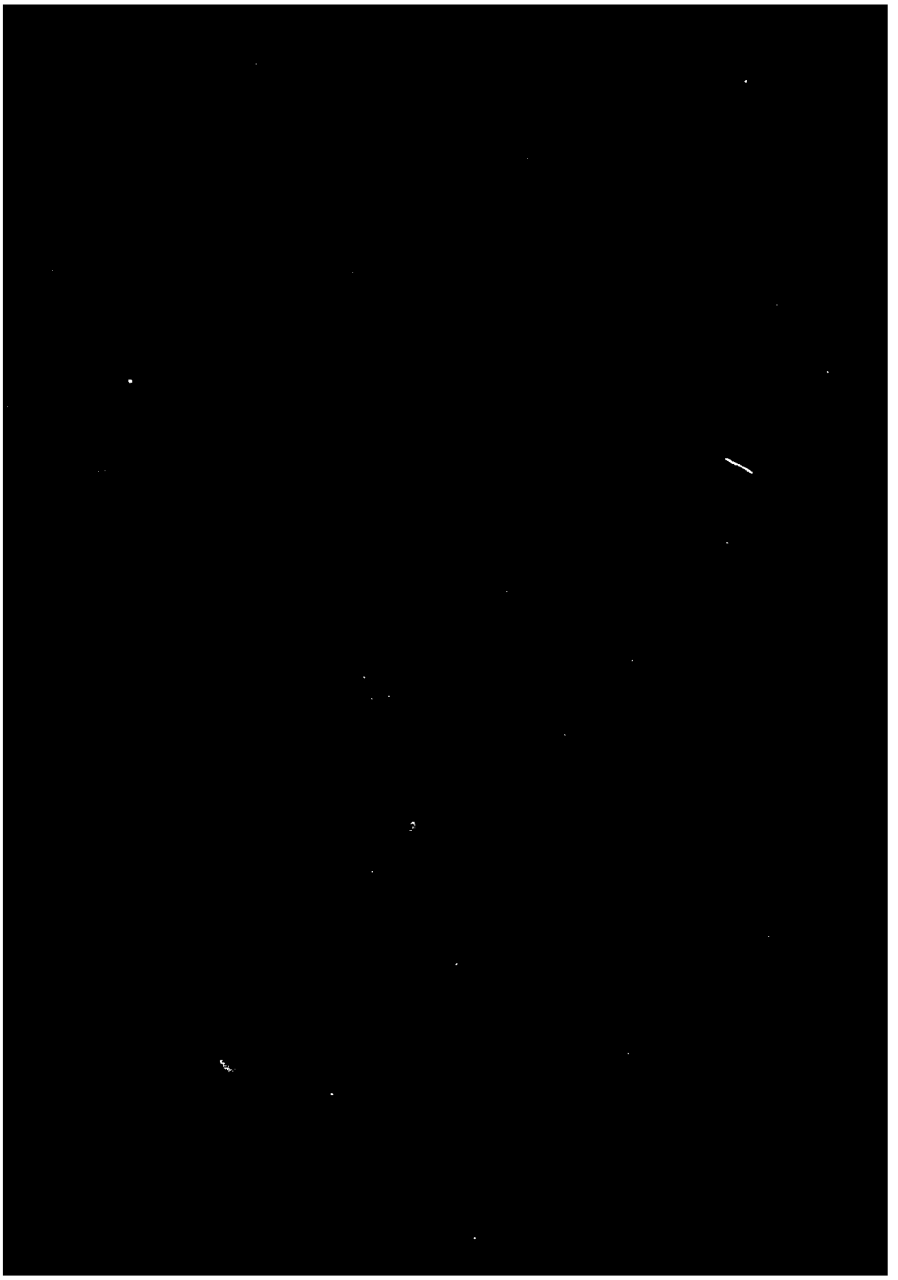

Unclassified

SECURITY CLASSIFICATION OF THIS PAGE (When Data Entered)

REPORT DOCUMENTATION PAGE	READ INSTRUCTIONS BEFORE COMPLETING FORM
1. REPORT NUMBER: AFOSR-TR-81-0676 / 2. GOVT ACCESSION NO.: AD-A105 403	3. RECIPIENT'S CATALOG NUMBER
4. TITLE (and Subtitle): FUNDAMENTALS OF MAGNETIC INTERACTIONS NEW APPROACHES TO THEORY AND EXPERIMENT.	5. TYPE OF REPORT & PERIOD COVERED: Final, 16 June 79 — 14 June 81
	6. PERFORMING ORG. REPORT NUMBER
7. AUTHOR(s): A. Lempicki, W.J. Miniscalco, B.C. McCollum, E.J. Johnson, R.M. Davies, S.J. Nettel, R.R. Gamache, N. Sanford	8. CONTRACT OR GRANT NUMBER(s): F49620-79-C-0182
9. PERFORMING ORGANIZATION NAME AND ADDRESS: GTE Laboratories, Inc. 40 Sylvan Road Waltham, Massachusetts 02254	10. PROGRAM ELEMENT, PROJECT, TASK AREA & WORK UNIT NUMBERS: 61102F 2301/A5
11. CONTROLLING OFFICE NAME AND ADDRESS: Air Force Office of Scientific Research Building 410 Bolling AFB, Washington, D.C. 20332	12. REPORT DATE: August 1981
	13. NUMBER OF PAGES: 68
14. MONITORING AGENCY NAME & ADDRESS (if different from Controlling Office)	15. SECURITY CLASS. (of this report): Unclassified
	15a. DECLASSIFICATION/DOWNGRADING SCHEDULE

16. DISTRIBUTION STATEMENT (of this Report)

Approved for public release; distribution unlimited.

17. DISTRIBUTION STATEMENT (of the abstract entered in Block 20, if different from Report)

18. SUPPLEMENTARY NOTES

19. KEY WORDS (Continue on reverse side if necessary and identify by block number)

magnetic semiconductors, cadmium chromium selenide, cadmium chromium sulfide, opto-magnetic effect, photo-magnetic effect, photo luminescence, magnetic interaction, superexchange RKKY interaction, band theory, OPW calculation, indirect exchange

20. ABSTRACT (Continue on reverse side if necessary and identify by block number)

Optically induced changes in magnetization (optomagnetism) have been observed for $CdCr_2Se_4$ and several other magnetic semiconductors. The effect has never been adequately explained although the most likely cause is RKKY coupling through optically excited carriers. Optomagnetism and other manifestations of carrier-spin interaction are intimately related to the electronic structure of these materials, particularly the narrow d and f bands. Realistic theories of these effects are lacking, in part because of the con-

DD FORM 1 JAN 73 1473

Unclassified

SECURITY CLASSIFICATION OF THIS PAGE (When Data Entered)

20. continued

troversy surrounding the electronic structure of many of these materials.

We report on the first stage of a joint university-industry, theoretical and experimental investigation of these effects in chromium chalcogenide spinels, particularly $CdCr_2Se_4$. This effort has involved a comprehensive investigation of their electronic structure, including an OPW band structure calculation and experimental photoluminescence and photoemission measurements.

Apparatus has been constructed to characterize optomagnetism using magneto-optic effects. Techniques for the growth of high quality, single crystal samples of $CdCr_2Se_4$ and $CdCr_2S_4$ have been developed and high quality crystals produced. The theoretical investigation of magnetic coupling in Cr spinels has resulted in new insights into the ground state magnetic coupling of these materials.

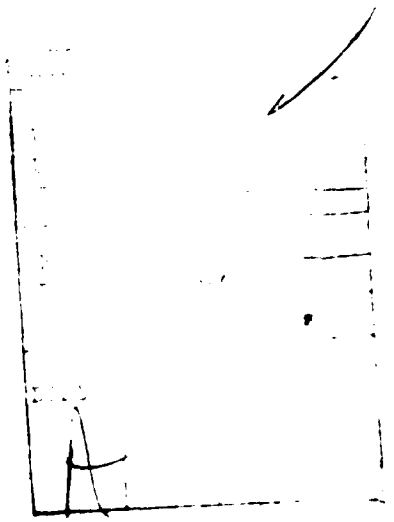

FUNDAMENTALS OF MAGNETIC INTERACTIONS
NEW APPROACHES TO THEORY AND EXPERIMENT

by

A. Lempicki
W.J. Miniscalco
B.C. McCollum
E.J. Johnson
R.W. Davies

R. Gamache
University of Lowell
Lowell, Massachusetts 01845

S.J. Nettel
N.Sanford
Rensselaer Polytechnic Institute
Troy, New York 12101

Final Report for Period
16 June 1979 — 14 June 1981

Contract No. F49620-79-C-0182

Prepared for:
Air Force Office of Scientific Research
Building 410
Bolling Air Force Base
Washington, D.C. 20332

15 August 1981

GTE LABORATORIES INCORPORATED
40 Sylvan Road
Waltham, Massachusetts 02254

TABLE OF CONTENTS

LIST OF ILLUSTRATIONS

Section 1
INTRODUCTION

Over the past three decades considerable progress has been made in the understanding of wide band metals and semiconductors. For materials containing narrow bands, however, the situation is quite different: in most instances the transport properties are not well understood and in a surprisingly large number of cases the electronic structure is still the subject of controversy. Belonging to this class of materials are magnetic semiconductors which are both of great physical interest and potentially of considerable technological importance. Typically, in these materials a rare earth or transition metal constituent contributes narrow bands either in addition to or instead of the wide, high mobility, s and p bands. These narrow f or d bands also result in magnetism and the magnetic and electronic properties of these materials are closely coupled. It is this interaction of the magnetic and electronic systems which gives rise to optically induced magnetization changes, the optomagnetic effect. The probable mechanism involves interband transitions which generate a significant carrier concentration which in turn alters the magnetic coupling via the RKKY interaction.

For more than a decade there has been considerable interest in the nature of magnetic coupling in semiconductors and how it is affected by illumination. We selected as the primary materials for the investigation of this subject the chromium chalcogenide spinel family of magnetic semiconductors which have the formula ACr_2X_4 (A=Zn, Cd, Hg; X=S, Se, Te). Among the reasons for this choice are the strong interaction between their electronic and magnetic systems and the observation of optomagnetic effects in $CdCr_2Se_4$. The work reported here concerns only the two best known Cr spinels, $CdCr_2Se_4$ and $CdCr_2S_4$.

Although chromium chalcogenide spinels, particularly $CdCr_2Se_4$ and $CdCr_2S_4$, have been extensively studied they are still poorly understood. The bulk of the work has been on two phenomena involving the coupling between the magnetic and electronic systems. The first concerns transport properties near the Curie temperature where resistivity and Seebeck coefficient anomalies[1,2] and negative magnetoresistance[1,3] are observed for n-type material. The second deals with the temperature and magnetic ordering dependent shifts of optical transitions.[4] These effects are manifestations of the influence magnetic ordering has upon the position

of the electronic states as well as the mobility of the excitations occupying them. The converse effect is the influence the electron and hole concentration have upon the magnetization and ordering temperature. This has been observed both as an equilibrium process through the dependence of the Curie temperature upon doping level [5,6] and as a transient process in which optical excitation produces changes in magnetization.[7]

Although several explanations of these effects have been proposed, none have been verified due to the lack of definitive experiments. Another stumbling block is that theoretical treatments require at least a qualitative knowledge of the electronic structure. The latter, however, has remained controversial due to the difficulty of interpreting the experiments and, until recently, the absence of band structure calculations. This situation has motivated us to undertake a self-contained program in which theory and experiment are to be done for both the optomagnetic effect and the basic electronic structure. The technical personnel who participated in this program are listed in Table 1.

TABLE 1

RESEARCH PERSONNEL

Name	Affiliation
Dr. A. Lempicki	GTE Laboratories (part time)
Dr. W.J. Miniscalco	GTE Laboratories (full time)
Dr. E.J. Johnson	GTE Laboratories (part time)
Dr. B.C. McCollum	GTE Laboratories (part time)
Dr. S. Nettel	RPI (part time)
N. Sanford	RPI (graduate student, full time)
Dr. R. Davies	U. of Lowell and GTE laboratories (part time)
Dr. R. Gamache	U. of Lowell (research associate, part time)

SECTION 2
RESEARCH OBJECTIVES

The program was divided into three efforts conducted by closely interacting research groups. The experimental work was conducted at GTE Laboratories while the theoretical investigations were performed at the University of Lowell and Rensselaer Polytechnic Institute (RPI).

2.1 EXPERIMENTAL EFFORT AT GTE LABORATORIES

1. Optical investigation of the electronic structure of Cr spinels.
2. Synchrotron radiation photoemission investigation of electronic structure.
3. Opto-magnetic measurements.
4. Growth and characterization of pure and doped Cr spinel crystals.
5. Investigation of other promising magnetic semiconductors.

2.2 RELATIVISTIC BAND STRUCTURE CALCULATION AT LOWELL

1. Work out group theory for spinel structure.
2. Assembly and debugging of relativistic OPW program.
3. Preliminary runs on known materials.
4. Preliminary band structure determination for $CdCr_2Se_4$.
5. Extension of results using k.p perturbation theory.
6. Programming for self-consistent calculation.

2.3 THEORETICAL EFFORT AT RPI

1. Investigate interrelationship of various indirect magnetic coupling schemes.
2. Investigate effect of spin-orbit coupling on conventional Heisenberg interaction.
3. Relate experimental observables to theory.
4. Develop quantitative theory of opto-magnetic effects.

SECTION 3
EXPERIMENTAL EFFORT AT GTE LABORATORIES

3.1 OPTICAL INVESTIGATION OF THE ELECTRONIC STRUCTURE OF Cr SPINELS

In addition to wide conduction and valence bands, chromium chalcogenide spinels contain narrow bands derived from the Cr 3d states. Two basic questions for such materials are what is the size of the fundamental gap (here defined as extending from the top of the valence band to the bottom of the conduction band), and where are the d-bands located relative to the wide bands and the Fermi level? Since the Cr sites have octahedral symmetry the d-states split (neglecting spin) into a three-fold degenerate t_{2g} level and a two-fold degenerate e_g level. To determine which of the four possible electronic structures illustrated in Figure 1 is correct, we undertook a series of photoluminescence and photoemission experiments. These investigations have revealed that the electronic structure of $CdCr_2Se_4$ and $CdCr_2S_4$ is that shown in Figure 2.

Our photoluminescence measurements resolved the long-standing controversy over the assignment of the valence band to conduction band transition and the size of the fundamental gap.[8] A reprint describing the work on $CdCr_2Se_4$ has been included as Appendix A. Optical techniques had located a large number of transitions but no consensus as to their identity had been arrived at. Although we are the first to report photoluminescence

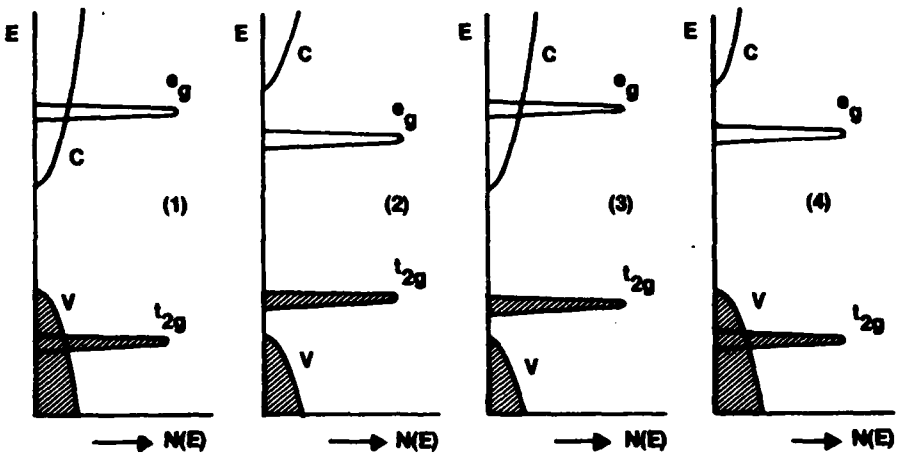

Figure 1. The four possible electronic structures for chromium chalcogenide spinels. The shaded states are occupied; the unshaded are unoccupied. Only the parallel spin d-bands are shown since the antiparallel ones are at much higher energy due to intra-Cr exchange.

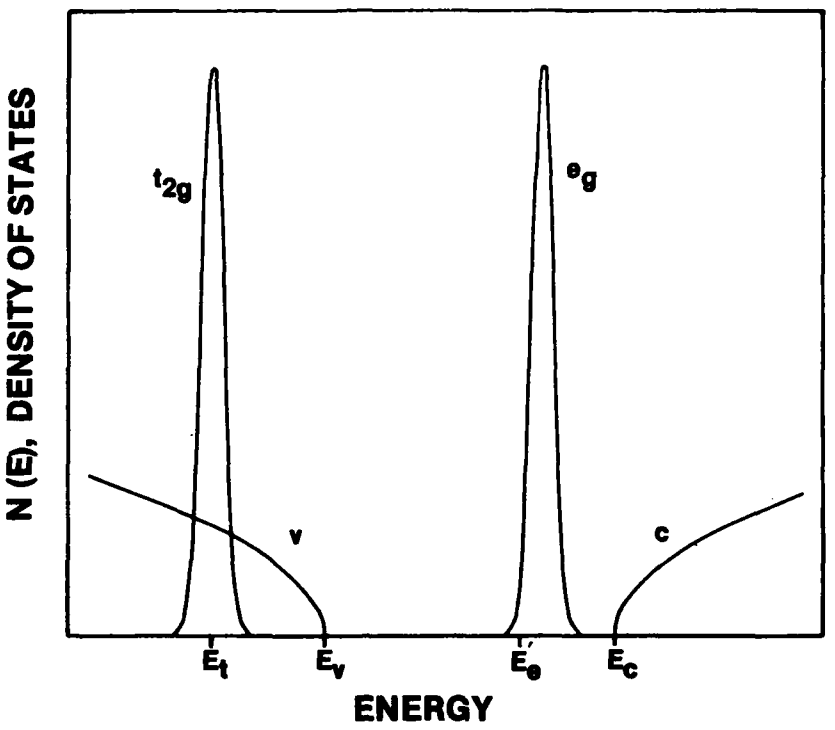

Figure 2. The correct electronic structure of $CdCr_2Se_4$ and $CdCr_2S_4$ based upon photoluminescence and photoemission measurements. The fundamental gap (E_c-E_v) is 1.8 eV for $CdCr_2Se_4$ and 2.5 eV for $CdCr_2S_4$. The distances below the top of the valence band for the filled t_{2g} d-bands (E_v-E_t) are 1.45 eV for $CdCr_2Se_4$ and 1.65 eV for $CdCr_2S_4$. The energy of the absorption edge is given by E'_e-E_v.

for $CdCr_2S_4$, it had previously been observed by Veselago et al.[9,10] for $CdCr_2Se_4$. The emission is difficult to interpret since it is at higher energy than the absorption edge, and these authors erroneously attributed it to transitions between crystal field split states of Cr^{3+}. Through a systematic investigation which included luminescence spectra and decay as a function of temperature as well as a determination of the quantum yield, we were able to demonstrate that the emission results from conduction band to valence band transitions. In addition to determining the size of the fundamental gap, we found that there must be a large number of states (probably d-bands) in the gap which cause both the long wavelength absorption edge and the fast relaxation of the wide band states. Accordingly, we were able to conclude that Case 1 of Fig. 1 is not a possible electronic structure for $CdCr_2Se_4$ or $CdCr_2S_4$.

3.2 SYNCHROTRON RADIATION PHOTOEMISSION INVESTIGATION FOR ELECTRONIC STRUCTURE

Using photoemission spectroscopy we have been able to eliminate Cases 2 and 3 of Figure 1 and arrive at the correct structure shown in Figure 2.[11] These measurements were performed on $CdCr_2Se_4$ and $CdCr_2S_4$ using synchrotron

radiation and are the first such investigation reported for chromium chalcogenide spinels. A preprint has been included as Appendix C. Photoemission measures the density of states on an absolute energy scale and is a powerful technique for locating structure in the valence band. The continuously variable photon energies available from a synchrotron source are particularly valuable for identifying features in the density of states. From its characteristic dependence on the energy of the exciting photon, a peak lying just below the top of the valence band in both materials was determined to be of d character. This resolved the question concerning the location of the occupied d-bands and placed them below the top of the valence band as indicated in Figure 2. These important results reveal that while electron conduction takes place in the narrow d-bands in the gap, hole conduction takes place in wide bands. This is another piece in the puzzle of why the interaction between the magnetic and electronic systems is only pronounced for n-type material.

3.3 OPTOMAGNETIC MEASUREMENTS

The first optically induced changes in magnetic properties for a semiconductor were reported for $CdCr_2Se_4$ by Lems et al.[12] in 1968. A similar effect has been observed for EuS[13] and the antiferromagnet $Cu_{1-x}In_xCr_2S_4$.[14] The two common procedures for measuring this effect are to use the sample as a transformer core[10] or to wind pickup coils on the sample.[14,15] Since these techniques are not capable of distinguishing magnetization changes from permeability or thermal effects, the results have been ambiguous. Proposed explanations of the effect include photoinduced pinning of domain walls,[16] changes in charge state through trapping of photogenerated carriers by either Cr ions or neighboring defect centers,[12,17] and alterations in the magnetic coupling strength by photogenerated carriers interacting with the spins via the RKKY interaction.[10,18,19] More direct evidence for optically induced magnetization changes has been provided by magnetic resonance on $CdCr_2Se_4$[7] and changes in absorption for EuS associated with magnetic ordering.[13] As a result of this work one can be quite certain that optically induced changes in magnetization do occur although domain wall pinning and thermal effects may play an important role as well.

Our general approach to characterizing the optomagnetic effect in Cr spinels is to measure the change in magnetization of a sample produced by optical excitation. The first technique used relied upon a Foner or vibrating sample magnetometer to measure the sample magnetization. However, difficulties were encountered in adapting the apparatus to low temperature operation. This technique was discontinued because the Foner magnetometer was only intended for preliminary investigations and the necessary modifications

would have required the same length of time as constructing the apparatus intended to supersede it. Accordingly, we proceeded directly to assembling the apparatus which uses magneto-optic effects to detect optically induced magnetization changes.

A material with a net magnetization exhibits the Faraday effect in which linearly polarized light propagating along the axis of magnetization suffers induced ellipticity with major and minor axes rotated with respect to the incident plane of polarization. When referring to reflected rather than transmitted light the phenomena is known as the magneto-optic Kerr effect. Both effects are extremely useful because the amount of rotation is proportional to the net magnetization. Faraday rotation is quite strong for $CdCr_2Se_4$ and $CdCr_2S_4$; absolute rotary powers of as much as 10^4 deg/cm have been observed for radiation near the absorption edge.[20] To these advantages of this technique is added the ability to work in the time domain and directly observe the dynamics of the optomagnetic effect.

A block diagram of the apparatus is shown in Figure 3. The linearly polarized probe beam is provided by a cw Nd:YAG laser at 1.06 micron; this wavelength is beyond the absorption edge of $CdCr_2Se_4$. The probe beam propagates through the sample along the axis of magnetization defined by an external magnetic field applied to align the domains. Figure 4 illustrates the steering prisms for the probe beam and the sample affixed to the cold finger of a variable temperature cryostat. The pulsed, tunable, optical

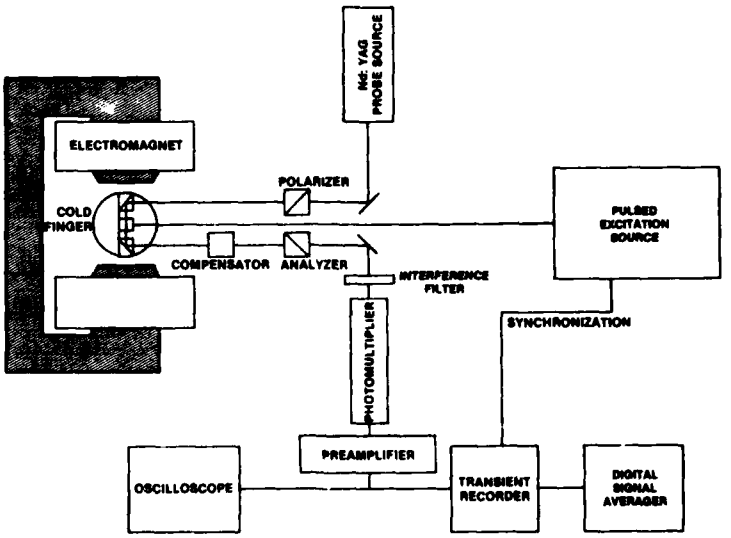

Figure 3. Block diagram of the apparatus to investigate the optomagnetic effect using Faraday rotation. The particular excitation source to be used depends upon the absorption and lifetime characteristics of the sample being studied.

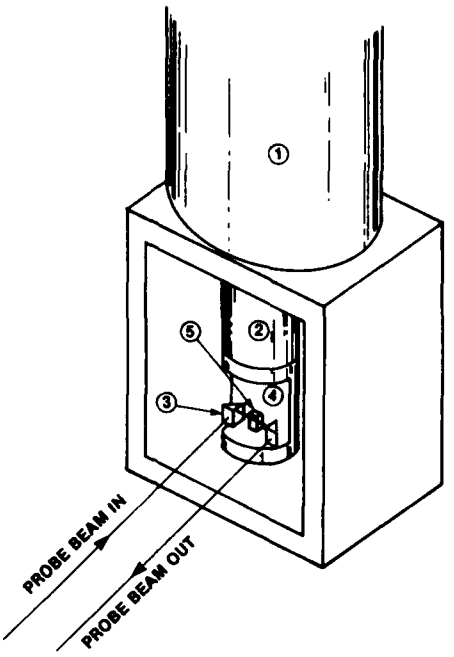

Figure 4. Sample holder and cryostat for use in the electromagnet. The labelled items are (1) cryostat vacuum shroud, (2) cold tip, (3) probe beam steering prisms, (4) sample holder, and (5) sample. The excitation beam is focused on front face of a sample and overlaps the volume interrogated by probe beam.

excitation is transverse to the probe beam and, depending upon the pulse width and energy requirements, is provided by a cavity dumped dye laser, Nd:YAG pumped dye laser, or a mode locked dye laser. Optically induced changes in magnetization alter the angle by which the sample rotates the plane of polarization of the probe beam and thereby change the amount of probe beam transmitted through the polarization analyzer.

The apparatus illustrated in Figure 3 has been constructed and is in the process of being tested. We have attempted to measure Faraday rotation for $CdCr_2Se_4$ and $CdCr_2S_4$ using a vector lock-in amplifier and a variable frequency optical chopper converted to a rotating polarizer. These investigations have been unsuccessful due to unexpectedly high absorption by both materials at 1.06 micron, the wavelength of the probe laser. Published absorption constants at this wavelength vary greatly for $CdCr_2Se_4$ and are very low for $CdCr_2S_4$. Accordingly we will be measuring the near-infrared absorption of both materials to determine if this probe wavelength can be used with samples of easily handled thicknesses. Currently we are developing grinding and polishing techniques to produce the ≤ 50 micron thick samples

necessary for the absorption and Faraday rotation measurements. A new superconducting solenoid will shortly replace the electromagnet and allow a much simpler experimental geometry than Figure 3.

3.4 CRYSTAL GROWTH

In any experimental investigation it is essential to have high-quality, well-characterized samples. Chromium chalcogenide spinels are not commercially available and it has been necessary for us to develop our own crystal growth program. This effort was started several years ago and we are now well along the learning curve for these difficult to produce materials.

In the course of this contract, some 50 separate experiments in the preparation of polycrystalline and single crystalline $CdCr_2S_4$ and $CdCr_2Se_4$ have been performed. This effort includes an initial growth of gallium doped $CdCr_2Se_4$ by a flux method.

Four principal methods have been reported for the growth of chromium chalcogenide spinel single crystals. These are by solid-state reaction,[21] vapor-liquid transport,[22] the flux method,[23] and chemical-vapor transport.[24] These techniques have been summarized in a review by Von Philipsborn.[25] Both the solid-state reaction and vapor-liquid transport methods were tried in the early stages of the contract period. Some very small (submillimeter) $CdCr_2Se_4$ crystals were obtained in an unreproducible manner, and these methods were dropped from further consideration.

Most of the effort in the growth program has been directed towards developing techniques for the flux growth of $CdCr_2Se_4$, our material of primary interest. Although the growth of magnetic spinels has been reported for quite some time, our experience suggests that reproducible crystal growth requires a learning period. The flux method, for example, requires commercially produced $CdCl_2$, CdSe, and $CrSe_x$ to be dried carefully before use. The stoichiometry of commercial "Cr_2Se_3" has been found to be unreliable. The material we used (from ICN) was analyzed and found to be 49.7 a/o Cr, that is, CrSe. Also, when using a $CdCl_2$ flux, the $CdCr_2Se_4$ spinel phase grows from a composition rich in Cd^{2+} and Cr^{3+} relative to Se^{2-}. The introduction of a thermal gradient along the quartz ampule during the growth process (following Prosser, et al.)[26] was found to bc quite helpful. We find, however, that the use of $CdCl_2$, CdSe, and $CrSe_x$ allows finer tuning of the growth composition than the reaction $2CrCl_3 + 4CdSe = CdCr_2Se_4 + 3CdCl_2$ reported by the above authors. Our melts, for best growth conditions, have been about 25% deficient in Se with respect to the Cr content with about 19 m/o "$CdCr_2Se_4$" based on the Cr content. Single crystal octahedra are now routinely 2 mm or more in size, with occasional larger crystals of good quality. Examples are illustrated in Figure 5.

The vapor transport method has been used to grow truncated $CrCr_2S_4$ octahedra of even better surface quality and larger size (Figure 6). Most of these are less than 1 mm thick by 2 to 4 mm across. They were grown using single phase polycrystalline $CdCr_2S_4$ spinel with $CrCl_3$ as the transport agent in a 935°C → 880°C thermal gradient. Stock polycrystalline $CdCr_2S_4$ was synthesized by heating stoichiometric quantities of well mixed CdS and Cr_2S_3 at 800°C for seven to 10 days in an evacuated quartz ampule. A typical vapor transport crystal growth run consisted of 3.0g of the polycrystalline $CdCr_2S_4$ (verified by X-ray diffraction patterns) with 60 to 100 mg of $CrCl_3$.

More recently, $CdCr_2Se_4$ has been grown successfully by the vapor transport method. In this case, preparation of polycrystalline $CdCr_2Se_4$ is complicated by the lack of commercial stoichiometric Cr_2Se_3. Accordingly, it was prepared as follows:

$$CdSe + 2Cr + 3Se \rightarrow CdCr_2Se_4$$

This reaction produces single phase product in an evacuated quartz ampule held at 860°C for seven to ten days. The vapor transport growth used 4.0g of $CdCr_2Se_4$ powder with 120 mg of $CdCl_2$ in a quartz ampule transported from about 770° → 720°C. The resulting crystals exhibit very nice surface facets. Most are truncated octahedra. Some are quite flat and others are nearly perfect small octahedra. The better crystals are 2 to 4 mm across a truncated triangular facet.

Figure 5. $CdCr_2Se_4$ produced by the $CdCl_2$ flux growth method. The single crystals are small octahedra 2-3 mm in size.

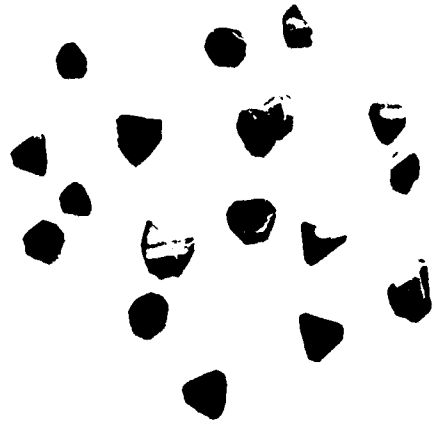

Figure 6. $CdCr_2S_4$ grown by the chemical vapor transport method. The single crystals are 2-4 mm across the large face.

The surface quality of the samples has been examined by scanning with an electron microprobe and observing the variation of Cd, Cr, Se, or S, and Cl. Early flux growth specimens were rather pitted and revealed observable variations in composition with occasional inclusions of Cl^-. More recent crystals showed no Cl^- and no compositional variation across the sample surfaces. The cubic spinel structure was verified by X-ray power patterns and spectrochemical analysis revealed only trace impurities. These tests indicate that our flux grown $CdCr_2Se_4$ and vapor transport grown $CdCr_2S_4$ are equal in size and quality to any reported in the literature.

SECTION 4
RELATIVISTIC BAND STRUCTURE CALCULATION

4.1 BACKGROUND

Theoretical calculations of the band structure of binary-compound, zinc-blende semiconductors have been numerous. In contrast, the present theoretical understanding of ternary-compound, spinel-type semiconductors is rudimentary. This is particularly the case for magnetic compounds such as $CdCr_2Se_4$ and $CdCr_2S_4$ where the structure of narrow 3d bands plays an important role.

One reason why the understanding of the spinel material has been limited is the large number of atoms per unit cell. In the case of $CdCr_2Se_4$ there are two formula units per unit cell, hence 14 atoms, as illustrated in Figure 7. This can be contrasted to a zinc-blende compound such as GaAs containing two atoms per unit cell. In turn, whereas the fundamental conduction and valence band states in GaAs can be specified by 8 orbitals (an s-like conduction band and a p-like valence band near the zone center), it typically requires 64 orbitals to specify the relevant conduction and valence bands in the spinel structure.[27]

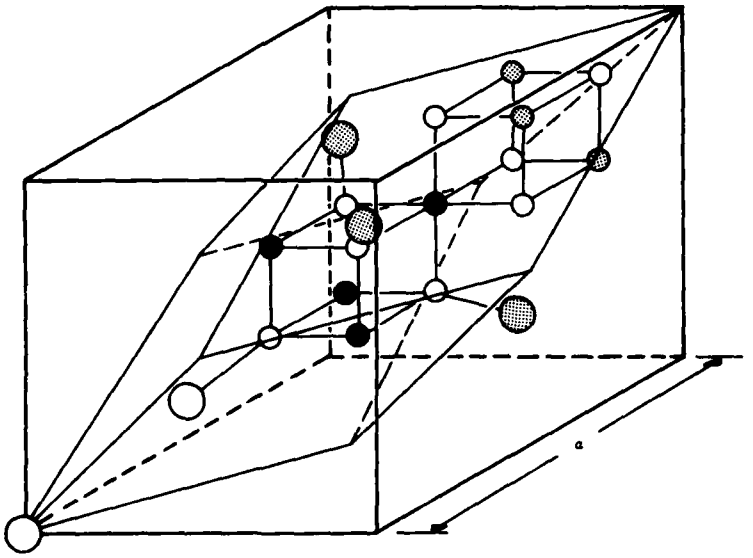

Figure 7. The spinel crystal structure. The primitive cell has lattice parameter a and contains two formula units. The large open and large flecked circles are Cd or Hg; filled-in and small flecked circles are Cr; small open circles are Se or S. The flecked circles are outside the unit cell.

Published band structure computations include model[27,28] and pseudopotential[29] calculations for the related non-magnetic spinels $CdIn_2S_4$ and $CdIn_2Se_4$. For the magnetic spinels $CdCr_2S_4$ and $CdCr_2Se_4$, calculations of the ferromagnetic band structure have been carried out using the extended Hückel[30] and the discrete variational Xα[31] techniques. The results from these methods have not been completely satisfactory. In particular, they yielded only qualitative agreement with experiment, and recent results from photoluminescence[8] and electron photoemission[11] investigations have uncovered details which are not entirely consistent with the published band structures.

One class of corrections which appears to have been neglected in previous calculations involves relativistic effects, particularly spin-orbit coupling. It is well known that the spin-orbit splitting of p-like valence states in moderately heavy-atom semiconductors can be appreciable. It seems clear that the spin-orbit splitting of the narrow d-bands in magnetic semiconductors should also be important. Considerations of this effect are needed, not only for the band structure, but also for computing Faraday and Kerr rotation constants, and for obtaining estimates of spin-relaxation times.

One reason for the importance of a fully relativistic band structure calculation is the following. Almost any ab initio band structure method makes use of the Xα local exchange approximation to the Foch self-energy. One then typically fixes the exchange constant (α) at the Slater[32] or Kohn-Sham[33] value, or with some experimental input, at a value which gives optimum agreement with the available data. However, for some time it has been recognized that relativistic effects (mass-velocity and Darwin corrections) can be substantial, and, in fact, can be as large or larger than differences resulting from the use of the Slater or Kohn-Sham α values. Even for Ge, which is relatively light, the relativistic correction[34] to the direct band-gap energy is about the same as the gap energy itself (0.8 eV). In view of these considerations, it is logical to include the relativistic effects in a rigorous fashion before worrying about the final adjustment of the exchange constant.

4.2 THEORETICAL PROGRESS

In August of 1979, we acquired a tape of a highly efficient, relativistic, self-consistent OPW code which was originally developed at Wright-Patterson Air Force Base[35] for energy-band calculations of zinc-blende semiconductors. A flow chart of the self-consistent procedure is illustrated in Figure 8.

FLOW CHART OF OPW METHOD

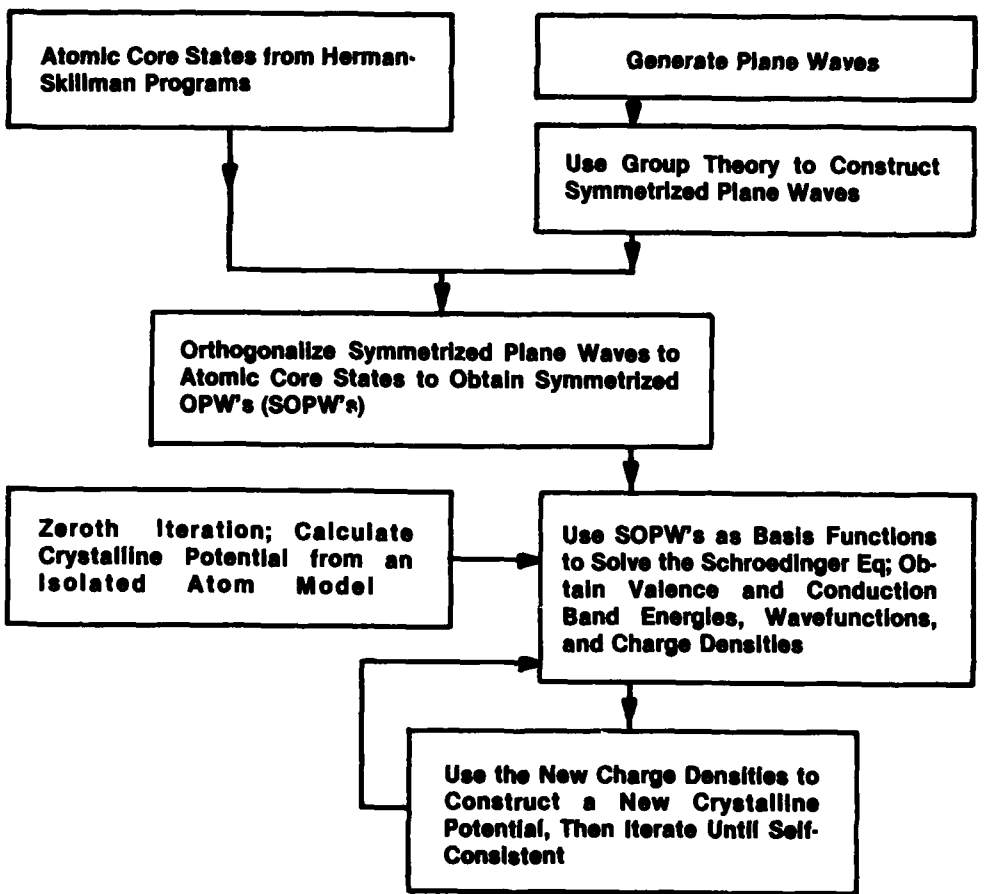

GTE

Figure 8. Flow Chart of OPW Method

Since that time, we have embarked on the task of converting the code from zinc-blende (T_d^2) space group symmetry to the spinel (O_h^7) symmetry. We have completed the group theory necessary to carry out this task, and all of the subroutines which make use of symmetry have been rewritten for the spinel structure. This task was complicated by the fact that O_h^7 is a non-symmorphic space group, containing nonprimitive translations as symmetry elements. A brief discussion of group representations for (double) non-symmorphic space groups is given in Section 4.3. Although character tables for the double group of O_h^7 (which is essentially the same as diamond, with a larger basis of atoms) have been published,[36,37] our method requires <u>all</u> the matrix elements of the group representations, and for the double group of O_h^7 these do not appear to be available. We have, therefore, constructed the irreducible representations by using direct products and other techniques. Matrix elements at six high symmetry points $\Gamma, X, L, W, \Delta, \Lambda$ are tabulated in Appendix E.

Because the contract did not extend the anticipated three year period, we have been unable to complete the rewriting of all necessary subroutines. However, we are nearing completion of the revisions of all subroutines necessary to carry out a non-self-consistent calculation for the spinel structure, and we expect to have some preliminary results by September of 1981.

We intend to continue work on this interesting subject, and items which will have high priority in the future include: (a) rewriting the subroutines which make the calculation self-consistent; (b) modifying the code to give a better treatment of d-states for magnetic semiconductors such as $CdCr_2Se_4$ by making use of the modified OPW method as developed by Deegan and Twose,[38] and by Butler, Bloom, and Brown,[39] (c) using calculated wave functions to evaluate overlap matrix elements for the indirect Rudermann-Kittel (RKKY) magnetic coupling scheme.

4.3 DOUBLE NONSYMMORPHIC GROUP THEORY FOR THE SPINEL STRUCTURE

There are essentially two ways of dealing with nonsymmorphic space groups: one is the factor group method,[40] the second makes use of ray representations.[41] We believe the latter is more convenient, and this is the method used by Slater,[42] who, however, does not express the method in these terms.

In the ray group method, one works only with symmetry elements of the form $\{R_i|\vec{\tau}(R_i)\}$ where R_i is a point group operation, and where $\tau(R_i)$ is a nonprimitive translation. These elements do not form a group in the usual sense. To have a group, one would also have to allow elements of the

form $\left\{R_i \mid \vec{\tau}(R_i)+r_n\right\}$, where $\vec{r}_n$ is a primitive translation. Nevertheless the simpler elements almost form a group in the sense that when operating on a plane wave $e^{i(\vec{k}+\vec{K})\cdot\vec{r}}$, one finds:

$$\left\{R_j \mid \vec{\tau}(R_j)\right\}\left\{R_i \mid \vec{\tau}(R_i)\right\} = \chi_{\vec{k}}(R_j,R_i)\left\{R_jR_i \mid \vec{\tau}(R_jR_i)\right\}, \tag{4.1}$$

where χ is a number which depends only on the reduced part $(\vec{k})$ of the wavevector and not on the reciprocal lattice vector $(\vec{K})$. The χ's also have the properties

$$|\chi_{\vec{k}}(R_j,R_i)| = 1 , \tag{4.2}$$

and for a given $\vec{k}$ (which is suppressed below)

$$\chi(R_j,R_j^{-1}R_i) = \chi(R_j,R_j^{-1})/\chi(R_j^{-1},R_i) . \tag{4.3}$$

These properties are associated with a ray space, and group representations (called ray representations)[41] satisfy the rule of multiplication

$$\Gamma\left\{R_j \mid \vec{\tau}(R_j)\right\}\Gamma\left\{R_i \mid \vec{\tau}(R_i)\right\} = \chi(R_j,R_i)\,\Gamma\left\{R_jR_i \mid \vec{\tau}(R_jR_i)\right\} \tag{4.4}$$

where the Γ's are (irreducible) square, unitary matrices. The $\chi(R_j,R_i)$ factors for O_h^7 have been tabulated in Table A3-19 of Slater's book.[42]

A symmetrized plane wave spinor corresponding to the u-th partner of a p-th irreducible representation is then constructed as

$$|\phi^{p}_{u\lambda}(\vec{k}+\vec{K})\rangle = P^{(p)}_{u\lambda}|\phi(\vec{k}+\vec{K})\rangle \tag{4.5}$$

where $|\phi(\vec{k}+\vec{K})\rangle$ is a sample plane wave spinor, and where P is a projection operation given by

$$P^{(p)}_{u\lambda} = \frac{l_p}{g}\sum_{R_i}\Gamma^{(p)}_{u\lambda}\left\{R_i \mid \vec{\tau}(R_i)\right\}\left\{R_i \mid \vec{\tau}(R_i)\right\} \tag{4.6}$$

Here in the relativistic case, the operator $\left\{R_i \mid \vec{\tau}(R_i)\right\}$ operates not only on the spacial part of the wavefunction, but also on the spin function, i.e., $\left\{R_i \mid \vec{\tau}(R_i)\right\}$ involves the Γ_6^+ representation operator as tabulated by Slater.[42]

Also in the relativistic case, the single group representations all project to zero,[40] hence only the "extra" representations of the double group, which have the property $\Gamma(\bar{R}_i) = -\Gamma(R_i)$, need to be considered.

In spite of the fact that the matrices of the non-symmorphic group multiply according to the "funny" rule, Equation (4.4), one can still show that they satisfy the "Great Orthogonality Theorem", and that the symmetrized plane waves generated by the procedure transform correctly, namely that they transform according to the rule[43]

$$\left\{R_j \mid \vec{\tau}(R_j)\right\} \mid \phi^{(p)}_{u\lambda}(\vec{k}+\vec{K})> = \sum_{\lambda''} \Gamma^{(p)}_{\lambda'' u}\left\{R_j \mid \vec{\tau}(R_j)\right\} \mid \phi^{(p)}_{\lambda'' \lambda}(\vec{k}+\vec{K}) \qquad (4.7)$$

Of course, the importance of symmetry is that it factors the Hamiltonian secular equation into blocks corresponding to different irreducible representations, and the Hamiltonian has no matrix elements between different partners of the same IR, and moreover, these matrix elements are independent of partner index.

Matrix elements for six high symmetry points for the double group of O_h are tabulated in Appendix E.

SECTION 5
THEORETICAL EFFORT AT RPI

The observation of the optomagnetic effect, the direct influence of light upon the magnetic structure, has been reported most frequently for $CdCr_2Se_4$.[7,12,15,17] The magnetic coupling in the chromium chalcogenide spinel semiconductors has traditionally been attributed to localized coupling in the form of superexchange.[44,45] The occurrence of optomagnetism in semiconductors has been variously attributed to domain wall pinning,[16] localized spin-transfer,[17] or itinerant electron (RKKY) magnetic coupling.[10,18,19] As a first step we have investigated the role of RKKY coupling resulting from virtually-excited electrons for the ground state coupling of $CdCr_2Se_4$, i.e. in the absence of real itinerant electrons. We found that superexchange is a fourth order effect that depends upon a small energy difference between spin-up and -down states of a Cr excited electron, and is small compared to the second-order RKKY coupling.

The magnetic coupling which we develop involves the indirect ferromagnetic interaction of Cr^{3+} ions mediated by an intervening Se atom. Authors in the past have presented similar schemes in attempts to come to grips with the problem of magnetic coupling.[44] However, these methods involve notions of localized atomic orbitals on individual Cr and Se atomic sites, and fail to give an adequate description incorporating the Bloch nature of the problem. Our method is a synthesis of both approaches and entails coupling magnetic Cr^{3+} ions via conduction electrons which result from virtual excitations from selenium valence band states.

We assign localized character to the Cr 3d ground state orbitals associated with the filled t_{2g} d-bands found below the top of the valence band in the photoemission measurements (Appendix C). On the other hand, we attribute Bloch character to the excited Cr wavefunctions which we identify with the unfilled e_g d-bands placed in the fundamental gap by band structure calculations.[30,31] These calculations show strong mixing of the excited d-states with Se p-states and lend further credence to our interpretation of these as extended Bloch states. Accordingly, the RKKY interaction depends on one-center coulomb exchange matrix elements and is expected to be a large effect compared to superexchange. Details are found in reprint included as Appendix B.

With the dominant ground state coupling in $CdCr_2Se_4$ established, it becomes a straightforward matter to identify the mechanism for optomagnetism. We find that the RKKY coupling between two Cr spins located at crystal sites $\vec{R}_A, \vec{R}_B$ is given by:

$$F(\vec{R}_A-\vec{R}_B) = \frac{1}{N} \sum_{k,k'} \left[\frac{\left\{ e^{i(\vec{k}-\vec{k}') \cdot (\vec{R}_A-\vec{R}_B)} \right\}}{E_{sek} - E_{crk'}} g_A g_B^* + c.c. \right] \qquad (5\text{-}1)$$

with

$$g_A = \int u_A^* \; (\vec{r}_1-\vec{R}_A)\, u_{cr}'^{s*} \; (\vec{r}_2-\vec{R}_A)\, u_{cr}' (\vec{r}_1-\vec{R}_A)\, u_A (\vec{r}_2-\vec{R}_A)\, (e^2/r_{12})\, d^3r_1 d^3r_2.$$

Here u_A refers to the localized ground state Cr orbital whose spin is being coupled, $u_{cr}'^{s}$ refers to that part of the Cr e_g orbital which is hybridized with the Se 3p orbitals to form the valence band, and u_{cr}' is the Bloch-symmetrized Cr e_g orbital to which the virtual excitations take place.

Appendix B discusses the two mechanisms by which RKKY coupling can produce optomagnetism. The most obvious is one in which the photoexcited electrons act as RKKY coupling electrons just as in metals. In the second effect, optical excitation produces interference with the ground state coupling. Owing to the Pauli exclusion principle, a many-electron treatment will show that those states occupied by a photoexcited electron must be excluded from the sum over excited states k' in Equation 3.5-1. As is explained in Appendix B, the interference effect is the larger of the two. With the wavefunctions and eigenvalues that will be produced by the OPW calculation, it will be possible to evaluate Equation 3.5-1 taking the interference effect into account and obtain a quantitative description of optomagnetism.

Our greatest interest is in calculating the shift of the Curie temperature with illumination, i.e., the Curie temperature as a function of free carrier concentration. Calculating the Curie temperature requires summing the interaction $F(\vec{R}_A-\vec{R}_B)$ between spins at sites $\vec{R}_A$ and $\vec{R}_B$ (Equation 2.5-1) over all lattice vectors $\vec{R} = \vec{R}_A-\vec{R}_B$. Prototype calculations of these sums have been reported by Woll and Nettel[46] and Mattis and Doniah.[47] Significant modifications to these approaches are required, however, because our problem differs in three important respects: i) The Cr sub-lattice in the chalcogenide spinels consists of <u>four</u> interpenetrating sc structures whereas previous calculations were for the hcp[46] and the three simple cubic structures.[47] ii) Our situation involves an energy gap in the energy denominator. There are a number of papers that consider the effect of a

gap, but none actually calculate the lattice sums.[48,49] iii) There will, in general, be a non-degenerate distribution of the photo-excited electrons in the d-band whose coupling effects we intend to calculate. This will require a temperature-dependent theory; a number of papers suggest how this can be done.[48,50]

To date we have succeeded in using the Holstein-Primakoff[51] approach to re-express the Heisenberg spin Hamiltonian for the spinel structure as a Fourier decomposition of spin wave frequencies. Diagonalization of this Hamiltonian is in progress and will yield the complete spin wave spectrum as a function of wave vector. Analysis of the resulting dispersion curves will give insight into the nature of the magnetic ordering and transition temperature since positive spin wave frequencies indicate ferromagnetic order. The inclusion of temperature and band gap effects do not introduce significant complications and we expect to publish the results of the complete calculation shortly.

SECTION 6
ACCOMPLISHMENTS

6.1 PUBLISHED PAPERS

"Photoluminescent Determination of the Fundamental Gap for the Ferromagnetic Semiconductor $CdCr_2Se_4$," S. S. Yao, F. Pellegrino, R. R. Alfano, W. J. Miniscalso, and A. Lempicki, Phys. Rev. Lett. 46, 558 (1981); reprinted as Appendix A.

"Magnetic Coupling and Photo-Ferromagnetism in $CdCr_2Se_4$," Norman Sanford and Stephen J. Nettel, J. Appl. Phys. in press; reprinted as Appendix B.

6.2 MANUSCRIPTS SUBMITTED FOR PUBLICATION OR IN PREPARATION

"Photoemission Determination of the Occupied d-Band Position for $CdCr_2Se_4$ and $CdCr_2S_4$," W. J. Miniscalco, B. C. McCollum, N. G. Stoffel, and G. Margaritondo, submitted to the rapid communications section of Phys. Rev. B; preprinted as Appendix C.

"Photoluminescent Spectra and Kinetic of $CdCr_2Se_4$ and $CdCr_2S_4$," W. J. Miniscalco, A. Lempicki, S. S. Yao, F. Pellegrino, and R. R. Alfano, to appear in a special issue of the Journal of Luminescence devoted to the proceedings of the International Conference on Luminescence, 1981; preprinted as Appendix D.

Additional experimental results and discussion of photoemission investigation of $CdCr_2Se_4$ and $CdCr_2S_4$, W. J. Miniscalco, N. G. Stoffel, and G. Margaritondo, manuscript in preparation for Phys. Rev. B.

6.3 PAPERS PRESENTED ORALLY

"Optical Investigations of Chromium Chalcogenide Spinel Magnetic Semiconductors," W. J. Miniscalco, seminar presented at The City College of New York, 13 Mar 81.

"Photoemission Spectroscopy of $CdCr_2Se_4$ and $CdCr_2S_4$," W. J. Miniscalco, A. Lempicki, G. Margaritondo, N. G. Stoffel, and A. D. Katnani, presented at the March 1981 meeting of the American Physical Society.

"Optical Investigations of Chromium Chalcogenide Spinel Magnetic Semiconductors," W. J. Miniscalco, seminar presented at Sandia National Laboratories, 23 Mar 81.

"Optical Techniques for the Investigation of Semiconductors," W. J. Miniscalco, seminar presented at the Raytheon Research Division, 15 Apr 1981.

"Photoluminescent Spectra and Kinetics of $CdCr_2Se_4$ and $CdCr_2S_4$," W. J. Miniscalco, A. Lempicki, S. S. Yao, F. Pellegrino, and R. R. Alfano, presented at the International Conference on Luminescence, Berlin, July 1981.

"Photoluminescent Spectra and Kinetics of $CdCr_2Se_4$ and $CdCr_2S_4$," W. J. Miniscalco, A. Lempicki, S. S. Yao, F. Pellegrino, and R. R. Alfano, presented at the Third Conference on Dynamical Processes in the Excited States of Ions and Molecules in Solids, Regensburg, July 1981.

SECTION 7
REFERENCES

1. H. W. Lehmann, Phys. Rev. 163, 488 (1967).

2. A. Amith, G. L. Gunsalus, J. Appl. Phys. 40, 1020 (1969).

3. C. Haas, A.M.J.G. van Run, P.F. Bongers, W. Alber, Solid State Commun. 5, 657 (1967).

4. G. Busch, B. Magyar, P. Wachter, Physics Lett. 23, 438 (1966); G. Harbeke, H. Pinch, Phys. Rev. Lett. 17, 1090 (1966).

5. A. A. Minakov, G. L. Vinogradova, K. M. Golant, V. H. Makhotkin, V. G. Veselago, Sov. Phys. Solid State 19, 1214 (1977).

6. A. Selmi, P. Gibart, L. Goldstein, J. Magn. Magn. Materials 15, 1285 (1980).

7. N. M. Salanskii, N. A. Drokin, Sov. Phys. Solid State 17, 205 (1975).

8. S. S. Yao, F. Pellegrino, R. R. Alfano, W. J. Miniscalco, A. Lempicki, Phys. Rev. Lett. 46, 558 (1981); reprinted as Appendix A.

9. V. G. Veselago, I. A. Damaskin, S. L. Pyshkin, S. I. Radautsan, V. E. Tézlévan, JETP Lett. 20, 149 (1974).

10. V. G. Veselago, Colloq. Int. C.N.R.S. 242, 295 (1974).

11. W. J. Miniscalco, B. C. McCollum, N. G. Stoffel, G. Margaritondo, to be published; preprinted as Appendix C.

12. W. Lems, P. J. Bongers, U. Enz, Phys. Rev. Lett. 21, 1643 (1968).

13. M. M. Afanas'ev, M. E. Kompan, I. A. Merkulov, JETP Lett. 23, 570 (1976).

14. W. K. Unger, phys. stat. sol. (a) 48, K89 (1978).

15. S. G. Rudov, V. G. Veselago, Sov. Phys. Solid State 21, 1875 (1979).

16. L. V. Anzina, V. G. Veselago, S. G. Rudov, JETP Lett. 23, 474 (1976).

17. V. G. Veselago, E. S. Vigeleva, G. I. Vinogradova, V. T. Kalinnikov, V. E. Makhotkin, JETP Lett. 15, 223 (1972).

18. W. Baltensperger, A. M. de Graaf, Helv. Phys. Acta 33, 881 (1960).

19. S. Methfessel, D. C. Mattis, in Handbuch der Physik, edited by H. P. J. Wijn (Springer-Verlag, Berlin, 1968), Vol. XVIII/1, pp. 389-562.

20. P. F. Bongers, G. Zanmarchi, Solid State Commun. 6, 291 (1968); D. Kuse, IBM J. Res. Devel. 14, 315 (1970); S. Wittekoek, G. Rinzema, phys. stat. sol. (b) 44, 849 (1970).

21. H. von Philipsborn, J. Applied Phys. 38, 955 (1967).

22. H. von Philipsborn, J. Crystal Growth 5, 135 (1969).

23. G. H. Larsen, A. W. Sleight, Phys. Lett. 28A, 203 (1968).

24. H. L. Pinch, S. B. Berger, J. Phys. Chem. Solids 29, 2091 (1968).

25. H. von Philipsborn, J. Crystal Growth 9, 296 (1971).

26. V. Prosser, P. Hlídek, P. Höschl, P. Polívka, M. Zvára, Czech. J. Phys. B 24, 1168 (1974).

27. W. Rehwald, Phys. Rev. 155, 861 (1967).

28. M. Inoue, M. Okazaki, Jpn. J. Phys. 36, 780 (1974).

29. F. Meloni, G. Mula, Phys. Rev. B 2, 392 (1970); S. Katsuri, Jpn. J. Phys. 33, 1561 (1972).

30. T. Kambara, T. Oguchi, K. I. Gondaira, J. Phys. C 13, 1493 (1980).

31. T. Oguchi, T. Kambara, K. I. Gondaira, Phys. Rev. B 22, 872 (1980).

32. J. C. Slater, Phys. Rev. 81, 385 (1951).

33. W. Kohn, L. J. Sham, Phys. Rev. 140, 1133 (1965).

34. F. Herman, R. L. Kortum, I. B. Ortenburger, J. P. Van Dyke, J. Phys. (Paris) 29, 62 (1968).

35. R. N. Euwema, D. J. Stukel, T. C. Collins, in Computational Methods in Band Theory, edited by P. Marcus (Plenum Press, New York), p. 82; G. G. Wepfer, T. C. Collins, R. M. Euwema, D. J. Stukel, ibid, p. 124; G. G. Wepfer, T. C. Collins, R. N. Euwema, Phys. Rev B 4, 1296 (1971).

36. R. J. Elliott, Phys. Rev. 96, 280 (1954).

37. G. F. Dresselhaus, Doc. Dissertation, Univ. of Cal., 1955.

38. R. A. Deegan, W. D. Twose, Phys. Rev. 164, 993 (1967).

39. F. A. Butler, F. K. Boom, Jr., E. Brown, Phys. Rev. 180, 744 (1969).

40. In Selected Topics in Solid State Phys, Vol. X, Ed. by E. P. Wohlforth: Group Theory and Electronic Energy Bands in Solids by V. F. Cornwell, American Elsevier Publishing Co., Inc., N.Y. (1969).

41. H. Weyl, The Theory of Groups and Quantum Mechanics, Dover Publications, Inc. (page 181).

42. J. C. Slater, Quantum Theory of Molecules and Solids, Vol. 2, McGraw Hill Book Co., N.Y. (1965).

43. M. Tinkham, Group Theory and Quantum Mechanics, McGraw Hill Book Co., N.Y., 1964 (page 23).

44. J. B. Goodenough, J. Phys. Chem. Solids 30, 261 (1969).

45. R. M. White, T. H. Geballe, in Solid State Physics, edited by F. Seitz, D. Turnbull, H. Ehrenreich (Academic Press, New York, 1979), Vol. 35.

46. E. J. Woll, S. J. Nettel, Phys. Rev. 123, 796 (1961).

47. D. Mattis, W. E. Donaih, Phys. Rev. 128, 1618 (1962); D. C. Mattis, The Theory of Magnetism, (Harper and Row, New York, 1965).

48. S. Lara, R. Moreira Xavier, C. A. Taft, J. Phys. Chem. Solids 39, 247 (1978)

49. N. Bloembergen, T. J. Rowland, Phys. Rev. 97, 1679 (1955); S. Lara, R. Moreira Xavier, C. A. Taft, J. Phys. Ehcm. Solids 38, 795 (1977); J. Ginter, J. Kossut, L. Swierkowski, phys. stat. sol. 96, 735 (1979).

50. B. V. Karpenko. A. A. Berdyshev. Sov. Phys. Solid State 5, 2494 (1964); A. Mauger, phys. stat. sol. (b) 84, 761 (1977).

51. T. Holstein, H. Primakoff, Phys. Rev. 58, 1095 (1940).

8. APPENDICES

Appendix A. Photoluminescent Determination of the Fundamental Gap for the Ferromagnetic Semiconductor $CdCr_2Se_4$

(Reprinted from Physical Review Letters)

Photoluminescent Determination of the Fundamental Gap for the Ferromagnetic Semiconductor $CdCr_2Se_4$

S. S. Yao, F. Pellegrino, and R. R. Alfano
Physics Department, The City College of New York, New York, New York 10031

and

W. J. Miniscalco and A. Lempicki
GTE Laboratories, Inc., Waltham, Massachusetts 02154

(Received 7 July 1980)

Photoluminescence has been used to elucidate the electronic structure of the ferromagnetic semiconductor $CdCr_2Se_4$. Luminescence spectra and decay have been measured and analyzed as a function of temperature and the quantum efficiency has been determined at 77 K. The data indicate that the observed emission results from conduction-band to valence-band transitions and place the fundamental gap at 1.8 eV.

PACS numbers: 78.55.Hx, 75.50.Dd

Chromium chalcogenide spinels have generated considerable interest because they present the opportunity to study magnetic interactions in systems where the itinerant-electron population is accessible to experimental control.[1,2] We report here the first photoluminescence decay and quantum efficiency measurements for any of these materials. In addition, we have obtained, for the first time, emission under cw excitation and have demonstrated that luminescence is observed for all pump wavelengths shorter than that of the emission. As a result of these measurements, we have determined that the fundamental gap E_g of $CdCr_2Se_4$ is 1.8 eV.

$CdCr_2Se_4$ orders ferromagnetically at 130 K and has attracted special attention because it displays optically induced permeability changes[3] and possibly magnetization changes as well.[4] Although this material has been extensively studied by a wide variety of optical and transport techniques, its electronic structure has remained controversial. Recently, two band-structure calculations have appeared which differ both in the size of the fundamental gap and in the position of the narrow *d* bands relative to the valence and conduction bands.[5,6] To clarify experimentally the electronic structure of this material, we have measured quantum efficiency at 77 K as well as luminescence decay, line shape, and line position as a function of temperature. Although 1.8-eV luminescence had previously been reported by Veselago *et al.*[7] for $CdCr_2Se_4$, these authors attributed it to transitions between crystal-field-split states of Cr^{3+} rather than band-gap emission. This luminescence is difficult to assign because the absorption edge lies at lower energy (1.2 eV at 77 K[8]). The analysis of our data, however, indicates that this emission is not due to an intra-Cr^{3+} transition but rather results from a parity allowed, conduction-band to valence-band transition (possibly involving a shallow donor or acceptor). Accordingly, we have been able to determine that the size of the fundamental gap is 1.8 eV.

The experiments were performed with use of cw, nanosecond-pulse, and picosecond-pulse excitation. For line-shape analysis, low power ($\lesssim 10$ mW) cw excitation was provided by the 488-nm line of an argon-ion laser. A nitrogen-laser-dye-laser system was used to probe the effect of varying the exciting wavelength over the interval 560–685 nm. With both these excitation sources the emission was analyzed with spectrometers and detected with conventional photomultipliers. In the decay measurements, picosecond excitation was provided by a frequency doubled (530 nm), mode-locked Nd:glass laser (pulse width $\simeq 6$ ps) with detection by a 10-ps-resolution streak camera used in combination with band-pass filters. Single crystals of $CdCr_2Se_4$ approximately 1 mm on a side were mounted in optical cryostats and cooled by flowing N_2 gas.

The samples were grown with use of the flux method[9] and the lattice parameter was verified by an x-ray powder pattern. Spectrochemical analysis revealed only trace impurities.

Several samples were subjected to electron microprobe analysis which revealed no significant variations in composition across the 1-mm faces.

Figure 1 illustrates the results of the luminescence decay measurements at temperatures from 77 to 250 K. The decays are exponential at all temperatures. The large uncertainties in the

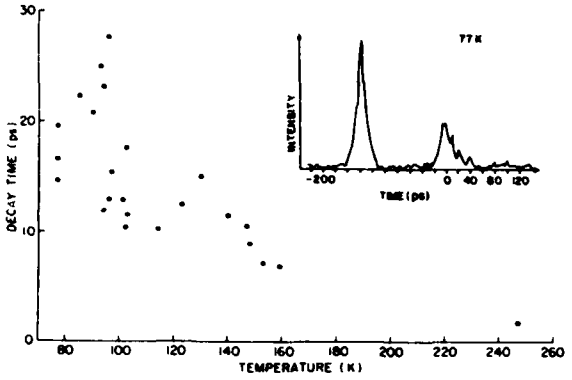

FIG. 1. Lifetime of $CdCr_2Se_4$ luminescence as a function of temperature. Decays are exponential at all temperatures and were measured at the emission peak (1.8 eV at 77 K). The inset shows a typical decay measurement.

shorter lifetimes are caused by the need to deconvolve the pulse width and streak tube response. The data show a clear pattern of an ~25 ps lifetime at 77 K falling to just a few picoseconds at room temperature. These very short lifetimes indicate that the relaxation of the excited state is dominated by nonradiative decay or transitions to intermediate states. This conclusion is confirmed by quantum efficiency measurements in which the emission intensity was compared to that of Rhodamine-6G under identical excitation and collection conditions. If we assume unit efficiency for Rhodamine-6G, the quantum efficiency of the 1.8-eV emission of $CdCr_2Se_4$ is 10^{-4} at 77 K. This value is probably an underestimate because of the strong self-absorption at this energy.

Taken together, these measurements reveal important information about the states involved in this transition. The quantum efficiency measurement indicates that at 77 K the radiative decay rate is $\geq 10^{-4}$ of the total decay rate, yielding a minimum value of 4×10^6 sec^{-1} for the radiative transition rate. This is too large for a parity forbidden transition and precludes the possibility of the transition being between crystal-field–split $3d^3$ states of Cr. In this material the Cr sites have octahedral symmetry[10] and in the many-electron representation the ground state of Cr^{3+} has $^4A_{2g}$ symmetry while the first excited state is either ^2E_g or $^4T_{2g}$.[11] In the high-crystal-field limit the former is lower making the transition to the ground state both spin and parity forbidden with typical radiative transition rates of $\simeq10^2$ sec^{-1}. In the low-field limit the $^4T_{2g}$ is the lowest excited state making the transition spin allowed with radiative rates $\simeq10^9$ sec^{-1}, still three orders of magnitude smaller than in $CdCr_2Se_4$. In the context of the more appropriate energy-band scheme, the 4×10^6 sec^{-1} rate for this material requires that the emission result from transitions between bands of opposite parity.

The decay measurements also clarify the ambiguities in electronic structure resulting from the absorption edge being at lower energy than the luminescence. As is the case for CdSe, one expects the band states and resonances to be strongly coupled to polar optical modes[12] and, therefore, to relax via intraband phonon-assisted processes on a time scale of less than a picosecond.[13] The observed decay time of 25 ps at 77 K requires a gap between the levels involved in the radiative transition and the lower-lying ones involved in the 1.2-eV absorption edge. The simplest interpretation of the optical data requires a 1.8-eV valence-band to conduction-band gap with d bands in the gap. The octahedral symmetry splits the Cr $3d^3$ states into two components with the Fermi level between them and one[6] or both[5] components in the gap. The absorption edge results from transitions between either occupied d bands in the gap and the conduction band or unoccupied d bands in the gap and the valence band. Emission results from conduction-band to valence-band transition. Both published calculations show some variation of this structure.[5,6]

To verify that we are observing fundamental-gap recombination we performed several additional tests, including line-shape analysis. Under moderate excitation nondegenerate free carriers in the conduction or valence band are described by a Maxwell-Boltzmann distribution.[12] For these conditions, interband recombination radiation reflects the Boltzmann factor, and the carrier temperature can be ascertained from an exponential fit to the high-energy edge of the line. This was done for spectra obtained under low-power cw excitation over the temperature interval from 90 to 200 K. The high-energy edges are exponential to within the accuracies of the measurements and Fig. 2 shows the calculated carrier temperature plotted as a function of the measured sample temperature. The good agreement indicates that free carriers thermalized to the lattice temperature are involved in this transition. At these high sample temperatures and low excitation levels the carrier temperature is expected to deviate little from that of the lattice.

The quadratic temperature dependence of E_g

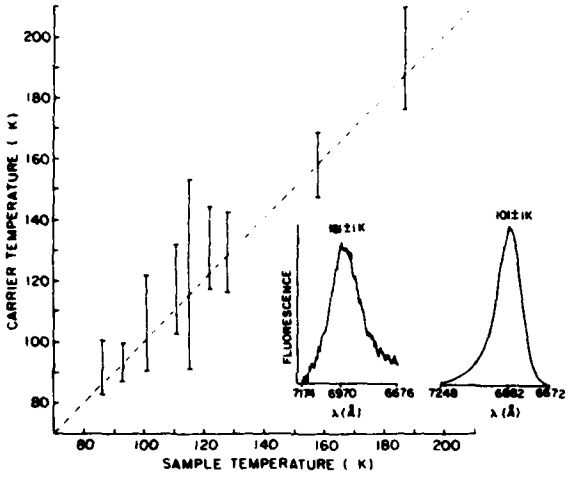

FIG. 2. Carrier temperature as a function of sample temperature. The carrier temperature T_c was obtained by fitting $\exp[-(E-E_g)/kT_c]$ to the high-energy edge of the recombination luminescence line. The dashed line corresponds to a carrier temperature equal to the sample temperature. The inset shows a typical emission spectrum.

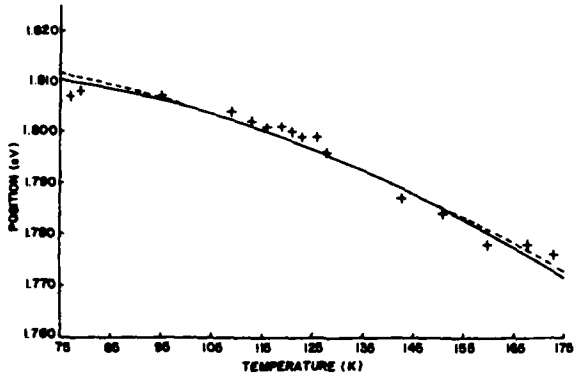

FIG. 3. Energy of the luminescence peak as a function of temperature. The lines are peak positions resulting from least-squares fits of E_g to a quadratic expression. The extreme values of the offset between emission peak and E_g are represented: the solid line is for a peak $2kT$ above E_g and the dashed line is for a peak $\frac{1}{2}kT$ above E_g.

for semiconductors at low temperature[14] has been used to further test our assignment of the 1.8-eV luminescence as band-gap emission. Figure 3 shows position versus temperature for the photoluminescence peak which demonstrates the expected behavior for E_g by shifting to lower energy as the temperature is increased. In contrast, the absorption edge shifts to higher energy with increasing temperature.[8] For allowed, interband recombination of noninteracting carriers the emission peak lies $\frac{1}{2}kT$ higher in energy than E_g for a direct transition and $2kT$ higher for an indirect transition. For both direct and indirect cases the electron-hole interaction will introduce an additive constant to the offset, while for the indirect transition it will in addition modify the offset so that it has no simple functional form but lies in the range from $\frac{1}{2}kT$ to $2kT$.[15] If either $\frac{1}{2}kT$ or $2kT$ is subtracted from the data of Fig. 3, the resulting values of E_g have a quadratic dependence on T. The peak position calculated by fitting E_g to a quadratic function is indicated for the $\frac{1}{2}kT$ and $2kT$ extreme cases by the lines in Fig. 3. The good agreement verifies that the temperature dependence of the luminescence is completely explained by a temperature dependence of the energy gap typical of nonmagnetic semiconductors. Unfortunately, the fits are not sensitive enough to determine where in the range from $\frac{1}{2}kT$ to $2kT$ the offset lies and give no information as to whether the transition is direct or indirect.

The above analyses, although establishing that a band must be involved in this emission, do not eliminate the possibility that the other state may be a deep level associated with an impurity or native defect. This situation would require the threshold for excitation to be a significant fraction of E_g larger than the emission energy. However, luminescence was excited with a dye laser tuned continuously over the range from 40 meV to 0.4 eV above the transition. The near-resonance excitation indicates that deep levels are not involved. Equipment limitations prevented a closer approach to resonance excitation, and so it is possible that the band gap is indirect or that shallow donors or acceptors are involved in the transition.

Our results are in qualitative agreement with the two recent theoretical band structures published for $CdCr_2Se_4$, and extended Hückel calculation by Kambara, Oguchi, and Gondaira[5] and a self-consistent $X\alpha$ calculation by Oguchi, Kambara, and Gondaira.[6] Kambara, Oguchi, and Gondaira predict a direct 1.7-eV fundamental gap for the ferromagnetic phase which is consistent with the value of 1.8 eV which we observe. Oguchi, Kambara, and Gondaira find a larger, slightly indirect gap of 2.3 eV. Although the emission energy is close to the separation at the

Γ point between the top of the valence band and the lowest antibonding *d* bands in the Oguchi calculation, the latter states have negative dispersion. Thus one would not expect to see emission from the bands at Γ but rather from the indirect minimum at X, a transition of only 0.7 eV. In addition to this quantitative discrepancy between our measurements and the $X\alpha$ calculation, another unresolved problem is the short carrier lifetime of this material. Nonradiative recombination or transitions to intermediate levels, possibly the *d* bands, are the dominant relaxation processes in $CdCr_2Se_4$. Like the deep levels in semi-insulating GaAs:Cr, the *d* bands in the gap may have the effect of shortening carrier lifetimes but to a much greater extend in this stochiometric material.

The crystals were grown by B. C. McCollum and D. Guenther. We wish to also acknowledge much helpful discussion with E. J. Johnson, S. J. Nettel, H. P. Hjalmarson, and R. W. Davies. Work at The City College of New York was supported in part by the Air Force Office of Scientific Research under Grant No. AFOSR-80-0079. Work at GTE Laboratories was supported in part by the Air Force Office of Scientific Research under Contract No. F49620-79-C-0182.

[1]C. Haas, CRC Crit. Rev. Solid State Sci. 1, 47 (1970).

[2]E. L. Nagaev, Usp. Fiz. Nauk. 117, 437 (1975) [Sov. Phys. Usp. 18, 863 (1976)]; W. Nolting, Phys. Status Solidi (b) 96, 11 (1979), and references therein.

[3]W. Lems, P. J. Rijnierse, P. F. Bongers, and U. Enz, Phys. Rev. Lett. 21, 1643 (1968); V. E. Makhotkin, G. I. Vinogradova, and V. G. Veselago, Pis'ma Zh. Eksp. Teor. Fiz. 28, 84 (1978) [JETP Lett. 28, 78 (1979)], and references therein.

[4]N. M. Salanskii and N. A. Drokin, Fiz. Tverd. Tela (Leningrad) 17, 331 (1975) [Sov. Phys. Solid State 17, 205 (1975)].

[5]T. Kambara, T. Oguchi, and K. I. Gondaira, J. Phys. C 13, 1493 (1980).

[6]T. Oguchi, T. Kambara, and K. I. Gondaira, Phys. Rev. B 22, 872 (1980).

[7]V. G. Veselago, I. A. Damaskin, S. L. Pyshkin, S. I. Radautsan, and V. E. Tézlévan, Pis'ma Zh. Eksp. Teor. Fiz. 20, 335 (1974) [JETP Lett. 20, 149 (1974)]; V. G. Veselago, Colloq. Int. C.N.R.S. 242, 295 (1974).

[8]G. Harbeke and H. W. Lehmann, Solid State Commun. 8, 1281 (1970); P. Hlidek, I. Barvik, V. Prosser, M. Vanecek, and M. Zvara, Phys. Status Solidi (b) 75, K45 (1976); B. Batlogg, M. Zvara, and P. Wachter, Solid State Commun. 28, 567 (1978), and references therein.

[9]V. Prosser, P. Hlidek, P. Hoschl, P. Polivka, and M. Zvara, Czech. J. Phys. B 24, 1168 (1974), and references therein.

[10]P. K. Baltzer, H. W. Lehmann, and M. Robbins, Phys. Rev. Lett. 15, 493 (1965).

[11]S. Sugano, Y. Tanabe, and H. Kamimura, *Multiplets of Transition-Metal Ions in Crystals* (Academic, New York, 1970).

[12]J. Shah, Phys. Rev. B 9, 562 (1974).

[13]C. V. Shank, R. L. Fork, R. F. Leheny, and J. Shah, Phys. Rev. Lett. 42, 112 (1979).

[14]G. D. Mahan, J. Phys. Chem. Solids 26, 751 (1965).

[15]R. J. Elliott, Phys. Rev. 108, 1384 (1957).

Appendix B. (Reprinted from Journal of Applied Physics)

MAGNETIC COUPLING AND PHOTO-FERROMAGNETISM IN $CdCr_2Se_4$

Norman Sanford[a] and Stephen J. Nettel
Department of Physics
Rensselaer Polytechnic Institute
Troy, New York 12180

a) GTE pre-doctoral fellow at GTE Laboratories, Waltham, MA 02254

ABSTRACT

We inquire as to a relation between the occurrence of photoferromagnetism in $CdCr_2Se_4$ and the mechanism of its ground-state ferromagnetic coupling. To explain the ground-state coupling we extend some of the localized orbital considerations of Goodenough to an itinerant electron coupling model. The coupling involves hybridized $Se\text{-}Cr^{2+}$ Bloch functions, with virtual excitations into the upper Cr-3d band. We find that there is reason to expect this coupling to be dominant over superexchange. We also find that the disturbance of this coupling by light is a major cause of the photoferromagnetism. The RKKY coupling is derived with the second-order pseudo-Hamiltonian of Pryce.

I. INTRODUCTION

Magnetic coupling in $CdCr_2Se_4$ is intriguing because a number of papers have reported the observation of photoferromagnetism (the influencing of magnetism by light) there.[1,2,3] Traditionally, magnetic coupling in thiospinel semi-conductors is attributed to superexchange, involving specified localized orbitals, including Cr^{3+} and Cr^{2+}-3d orbitals in the case of $CdCr_2Se_4$.[4] The occurrence of photo-ferromagnetism in semiconductors has often been linked with itinerant electron or RKKY magnetic coupling.[5,6] It will be recalled that the RKKY coupling for a lattice of spins is exceptionally sensitive to conduction band occupation. One finds that the magnetic interaction energy oscillates rapidly as a function of the Fermi radius.[7,8] Lastly, we note that very recent measurements on $CdCr_2Se_4$ by S.S. Yao et al.[9] have found life-times for conduction electrons of the order of 10^{-11} sec. at the 130°K Curie temperature, so short as to preclude any role for the conduction electrons in the magnetic coupling.

The emphasis on RKKY has led us to inquire into the role generally of itinerant electron coupling in the ground-state of $CdCr_2Se_4$, and its relationship to photo-ferromagnetism.

The present note suggests a simple way of incorporating some of the localized-orbital considerations of Goodenough into an itinerant-electron coupling mechanism. The model relies on the excited Cr^{2+}-d electron band rather than the Cr-4s conduction band. It utilizes the electronic structure of the very recent band calculation of Kambara et al. on $CdCr_2Se_4$ and $CdCr_2S_4$,[10] reinforced by the measurements of S.S. Yao et al.[9] to correlate ground-state magnetic coupling with the onset of photo-ferromagnetism.

II. MAGNETIC COUPLING MODEL

According to Goodenough there are two components to each near-neighboring Cr^{3+}-Cr^{3+} interaction, an antiferromagnetic cation-cation interaction due to overlapping of the half-filled t_{2g} orbitals (Fig. 1, see also Reference 4), and a ferromagnetic 90° cation-anion-cation interaction due to half-filled t_{2g} orbitals interacting indirectly with empty e_g orbitals on neighboring atoms. Our treatment will supplement only the latter interaction.

Spin-orbit interactions aside, the coupling of electronic spins arises from the well-known fact that exchange matrix elements of the coulomb interaction e^2/r_{ij} can only link orbitals of the same spin. Given the tedium of higher-order time independent perturbation theory for many particles, magnetic exchange coupling becomes complicated. We have found very helpful the treatise by Zeiger and Pratt, where some of the many possible ground and

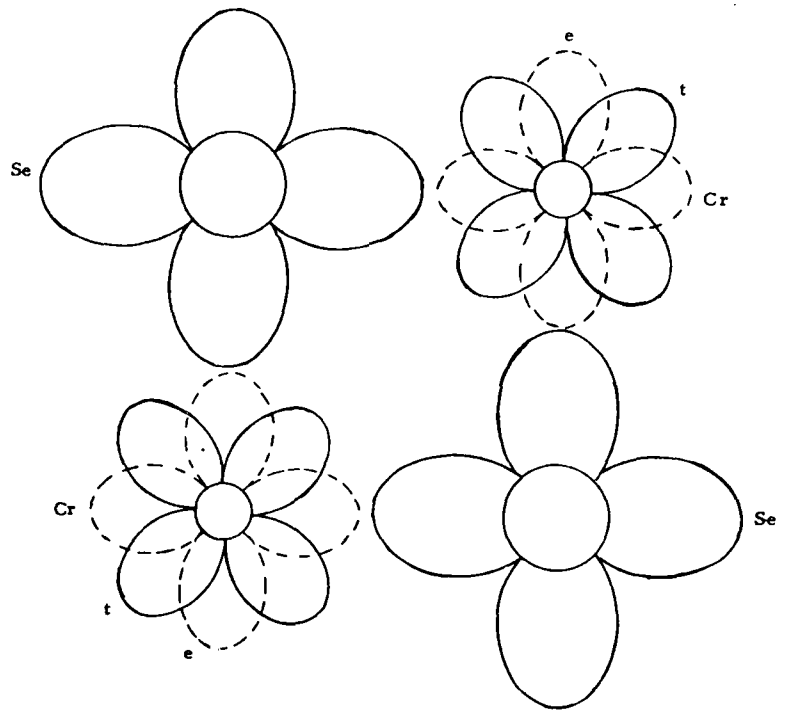

Fig. 1. Adjacent chromium and selenium ions. In the RKKY scheme selenium 3-p orbitals are taken to hybridize only with the empty Cr-e orbitals. The latter then exchange interact with the filled t orbitals.

associated excited states are represented by simple diagrams.[11] It seemed to us that one ought first to investigate qualitatively and quantitatively all possible second-order mechanisms, before resorting to the third order ones, such as superexchange. (The stricture of a theorem due to Kramers against second-order coupling mechanisms is now seldom heeded; usually there are many extra implicit interactions involved, for example, in our work in the hybridization of selenium orbitals, see below.) Thus, we were led directly to the RKKY magnetic coupling model of the next paragraph. It is based on the most effective of second-order Zeiger-Pratt diagrams for localized orbitals.

In Fig. 2 we show schematically the band structure of $Cd_2Cr_2Se_4$ as found by Kambara et. al. and reinforced by the photoluminescence measurements.[9]

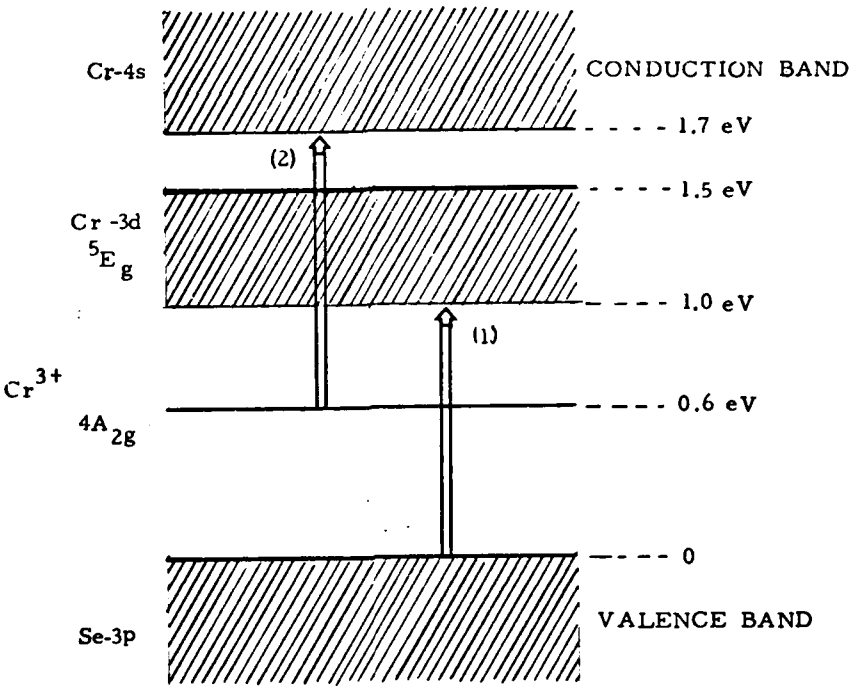

Fig. 2. Band-structure of $Cd_2Cr_2Se_4$ as found in the calculations of Kambara et al. (Reference 10), and confirmed by the photo-luminescence measurements of S.S. Yao et al. (Reference 9).

We see that while the $Cr^{3+}(^4Ag)$ band is narrow, the band deriving from the $Cr^{2+}(^5E_g)$ orbitals is not. We, therefore, continue to regard the Cr^{3+} electrons as localized, but write the higher lying Cr-3d electrons in Bloch form. The RKKY coupling of the localized Cr^{3+} spins is by the selenium valence electrons, excited into the empty upper Cr-3d Bloch state at the site of one spin and de-excited at the other.

The photo-ferromagnetism has its threshold at around 1.2 ev. Consequently, it is believed to involve either Process (1) or Process (2) in Figure 2.[14] Because (4s) electrons are so short-lived we can assume that most of those excited by Process (2) also spend their excited life-times in the empty upper chromium band. The optically excited electrons will affect the magnetic coupling in two partially related ways. The first and more obvious is the RKKY coupling which they provide on their own merit while occupying states in the excited Cr band, the same situation as encountered in an RKKY metal. The second is by exercising a Pauli exclusion blocking action on the virtual excitations of the selenium 3-p orbitals involved in the RKKY ground-state coupling and by the creation of selenium valence band holes. In "Conclusions" we argue that the second effects are probably the greater.

III. RKKY CALCULATION WITH BLOCH STATES

We start with the second-order perturbation theory quasi-hamiltonian as given by Pryce[13].

$$H_2 = -\sum_{n\neq o} \frac{P_o H^1 P_n H^1 P_o}{E_n - E_o} \tag{1A}$$

Here

$$H^1 = (e^2/r_{ij})(1/2 + 2s_i \cdot s_j) \tag{1B}$$

$$P_o, P_n = \left|o><o\right|, \left|n><n\right| \tag{1C}$$

In Eq. (1B) we have taken cognizance of the fact that only the exchange terms will contribute to the magnetic interaction between spins at site A and site B. The spin exchange operator has the form shown,[11] as one can verify by direct calculation of possible elements. P_o, P_n are projection operators, the manifold of states n, n = 0,1,2, corresponding to the ground and the two-excited states of the selenium electrons, see Fig. 3. The Cr^{3+} configurations, i.e., the spins on sites A, B, do not belong to the manifold. Equation (1A) is valid when we have degeneracy in the absence of the perturbation, the parallel and anti-parallel configurations are assumed to have the same energy for both excited states of Fig. 3, i.e., for n = 1,2. This is the necessary and sufficient condition for Equation (1A) and the resulting RKKY formula to hold.

We have in mind to apply the present scheme to a calculation with magnetic machine generated Bloch functions, which already contain all non-magnetic coulomb interactions, so that only the $s_i \cdot s_j$ term in Eq. (1B) concerns us.

We have from Eq. (1A)

$$H_2 = -4 \sum_{n=1,2} \frac{\left|o><o\right| (e^2/r_{ij}) s_i \cdot s_j \left|n><n\right| (e^2/r_{ij}) s_i \cdot s_j \left|o><o\right|}{E_n - E_o} \tag{2}$$

Keeping in mind that we have restricted ourselves to exchange terms and that the excited states n are given by Figure 3, we have

$$H_2 = 4(G_{ACC'A}s_A+G_{BCC'B}s_B)\sum_{n=1,2}\left|o><o\right|s_j\left|n><n\right|s_j\left|o><o\right|$$

$$X\ (G^*_{ACC'A}s_A+G^*_{BCC'B}s_B)/(E_n-E_o) \qquad (3A)$$

where we have transferred the spin suffixes from the electron to the orbital designation for the localized orbitals, and

$$G_{ACC'A}=\iint\phi^*_A(1)\phi^*_C(2)\phi_{C'}(1)\phi_A(2)(e^2/r_{12})dr_1dr_2 \qquad (3B)$$

Lastly, noting that

$$<o\left|s_x^2\right|o>=<o\left|s_y^2\right|o>=<o\left|s_x^2\right|o>=1/4$$

and that

$$<o\left|s_xs_y+s_ys_x\right|o> = \text{etc.} = 0$$

for a singlet state, and, restricting ourselves to terms coupling spins A and B we get:

$$H_2 = (G_{ACC'A}G^*_{BCC'B}+G_{BCC'B}G^*_{ACC'A})/(E_n-E_o)s_A\cdot s_B\left|o><o\right| \qquad (4)$$

where $\left|o>,<o\right|$ refers to singlet selenium states, and will be omitted hereafter.

To illustrate our argument we now write most simply for the selenium valence electrons:

$$\phi_c(1) = 1/\sqrt{N}\ \sum_{R_{se}} e^{ik\cdot R_{se}}\ u_{se}(r_1-R_{se})$$

$$+\ 1/\sqrt{N}\ \sum_{R_{cr}} e^{ik\cdot R_{cr}}\ U^{s}_{cr}(r_1-R_{cr}) \qquad (5A)$$

where the R_{se}, R_{cr} denote all selenium and chromium sites, and in reality the localized orbitals u_{se}, u^{s}_{cr} contain phase-factors that arise from their being two formula units in every unit cell of $CdCr_2Se_4$. Equation (5A) recognizes that the selenium wavefunctions hybridize with Cr^{2+} excited chromium orbitals, (u'^{s}_{cr}). We are not showing the selenium-chromium coupling constants which reduce somewhat the amplitudes contained in u'^{s}_{cr}. N is the number of unit cells in the crystal. For the excited Cr^{2+} band it suffices to write

$$\phi_{C'}(1) = 1/\sqrt{N}\sum_{R_{cr}} e^{ik'\cdot R_{cr}}\, u'_{cr}(r_1-R_{cr}) \tag{5B}$$

and for the localized unexcited 3-d chromium orbitals

$$\phi_A(1) = u_A(r_1-R_A) \qquad \phi_B(1) = u_B(r_1-R_b) \tag{5C}$$

Substitution of Eqs. (5) into Eqs. (3B) and (4) yields:

$$H_2 = 1/2 \sum_{A,B} F(R_A-R_B)\, s_A\cdot s_B \tag{6A}$$

$$F(R_A-R_B) = \frac{1}{N}\sum_{k,k'}\left[\frac{e^{i(k-k')\cdot(R_A-R_B)}}{E_{sek}-E_{crk'}}\, g_A g_B^{*} + c.c.\right] \tag{6B}$$

with

$$g_A = \int u_A^{*}(r_1-R_A)\, u'^{s*}_{cr}(r_2-R_A)\, u'_{cr}(r_1-R_A)\, u_A(r_2-R_A)\,(e^2/r_{12})\,dr_1 dr_2 \tag{6C}$$

and g_B formally the same matrix element computed at site B. To arrive at Eq. (6) we have had to enlarge the spin-manifold representing intermediate states by including all possible electron-hole pairs, k,k'. The degeneracy need exist only between different selenium spin configurations for the same electron-hole pair. Thus the sum on k in Eq (6) is on all occupied selenium Bloch orbitals, the sum on k' on all unoccupied excited Cr^{2+} orbitals. E_{sek} represents the energy of the former, $E_{crk'}$ of the latter orbitals. Also, in deriving Eq. (6A) we have restricted ourselves to the one-center coulomb matrix elements.

CONCLUSIONS

Equation (6) represents RKKY coupling of localized Cr^{3+} spins by selenium valence electrons, excited into the empty upper Cr-3d band at the site of one spin and deexcited at the other. The coupling of excited chromium orbitals to selenium orbitals in Eq. (5A) is via a σ-bond between the Se^{-2}p-orbital and the Cr^{2+}e orbital. This is one of the bonds singled out by Goodenough and by Kanamori[14] for the discussion of magnetism in a range of related compounds. The possibility of a synthesis between localized and RKKY coupling schemes was already considered by J. Ginter et al.[15] The coupling is now no longer restricted to near neighbors, but is long range. As mentioned in the Introduction a blocking action is introduced into the virtual excitations of Eq. (6B) by optically excited electrons. In a many electron treatment one sees that from the sum over k' in that equation any states occupied by photo-electrons must be omitted, - the result of the Pauli exclusion principle. By symmetry we see that this is equivalent in its effect on coupling to creating holes in the occupied portion of the coupling band. (The restriction, to vertical virtual processes in the case of ferromagnetism, see below, makes this equivalence even more evident.) The special magnetic sensitivity to electron occupation of the coupling band encountered with RKKY[5,15,16] here then leads to light sensitivity as a result of blocking of virtual Cr-3d excitations, as well as the optical formation of valence band holes.

In addition, as stated in the Introduction, one must consider the contribution to photoferromagnetism by the electrons optically excited into the upper chromium band giving magnetic coupling on their own merit, i.e., acting like coupling electrons in the partially filled conduction band of a metal. Because here there is no obvious band gap in the denominators of Eq. (6B), one might suppose that these electrons are more effective at coupling. However, we note that for a ferromagnetic lattice, the magnetic interaction of one spin with all the others involves a sum over lattice spin sites, S, given by

$$S = \sum_{B} F(R_A - R_B) \qquad (7)$$

It follows that virtual transitions in Eq. (6B) which contribute to S are limited to having (k-k') be a reciprocal lattice vector in a free electron picture[8,17], and here implies vertical processes on a reduced band scheme. As a result the denominators remain of the order of band separations.

Further, as regards what is probably the most important of these virtual vertical processes for the excited chromium electrons, namely those to the selenium valence band, they are blocked by the exclusion principle. For this reason we suspect the blocking action exerted by the excited Cr-3d electrons, as it affects the RKKY coupling of the ground state of the material, is probably the larger optical effect.

In comparing the RKKY coupling with that due to other known localized mechanisms we notice that the latter generally are formally at least of third order in perturbation theory.[11] Super-exchange depends upon an energy difference that arises in a third order expression,[18] (it is, thus, a fourth order effect). This energy difference itself corresponds to spin up and down of the excited Cr^{2+} electron, and, presumably is small on a scale of Cr^{2+}, Cr^{3+} band slitting. Indeed, we have neglected it in our formulation. On the other hand there is no reason why the one-center coulomb exchange terms appearing in the second order expression of Eq. (6B) should be small relative to band splitting, ($\simeq$ lev.) Finally, one needs to inquire as to the extent to which Cr_2^+ excited orbitals are coupled into the selenium valence-electron Bloch states. Kambara et al. in their energy band calculations found ionicities of $Cr^{1.94}$ $(Cr^{1.82})_2$ $(Se^{-1.39})_4$ as compared to the fully ionized configuration $Cd^{+2}(Cr^{+3})_2(Se^{-2})_4$. This strong hybridization is likewise evident from the "repulsion" between the upper chromium and the selenium band. Thus, the Cr^{2+}3d-Se^{2-}3p coupling can in practice be regarded as of order unity. All these considerations put together raise the very real possibility that the explanation for the occurrence of photoferromagnetism in $CdCr_2Se_4$ lies with the Cr^{2+} itinerant electron coupling proposed here.

Lastly we note that the interconnection between the RKKY magnetism of the ground state and photoferromagnetism may allow one to estimate the latter in terms of magnetic parameters characterizing the ground state. At the same time a careful machine calculation of $CdCr_2Se_4$ based on a paramagnetic state is now underway.[19] This will make available to us sufficiently realistic Bloch orbitals to allow us to evaluate the magnetic coupling and optomagnetic response of the model from first principles.

ACKNOWLEDGMENTS

We are deeply grateful to W. Miniscalco and A. Lempicki of GTE Labs for making available to us the results of their measurements with S.S. Yao, F. Pellegrino and R.R. Alfano of City College of New York prior to their publication. We are very much indebted to our colleagues working with us on opto-magnetism, W. Miniscalco, E.J. Johnson and A. Lempicki, at GTE Labs, and R.W. Davies of Lowell University for a number of very helpful discussions. Both writers wish to acknowledge the hospitality of the GTE Waltham Labs on numerous occasions. This work was supported by a subcontract from GTE Labs Inc. as part of AFOSR contract number F49620-79-C-0182.

REFERENCES

1. W. Lems, P.J. Rijnierse, P.F. Bongers and U. Enz, Phys. Rev. Letters 21, 1643 (1968)

2. V.G. Veselago, E.S. Vigeleva, G.J. Vinogradova, V.T. Kallinnikov and V.E. Makhotkim, JETP Letters 15, 223 (1972)

3. N.M. Salanskii and N.A. Drokin, Sov. Phys. Solid State 17, 205 (1975)

4. J.B. Goodeneough, J. Phys. Chem. Solids 30, 261 (1969)

5. S. Methfessel and D.C. Mattis, Handbuch der Phys. XVIII/I, Springer, NY (1968)

6. A.A. Berdyshev, Sov. Phys. Sol. Stat. 8, 1104 (1966)

7. The Theory of Magnetism, D.C. Mattis, Harper & Row, (New York, 1965), p. 201

8. E.J. Woll and S.J. Nettel, Phys. Rev. 123, 796 (1961)

9. S.S. Yao, F. Pellegrino, R.R. Alfano, W.J. Miniscalco and A. Lempicki (unpublished).

10. T. Kambara, T. Oguchi, and K.I. Gondaira, J. Phys. C., 13, 1493 (1980)

11. H.J. Zeiger and G.W. Pratt, Magnetic Interactions in Solids, Clarendon Press, (Oxford, 1973), p. 240

12. W.J. Miniscalco, private communication, see also Reference 9

13. M.H.L. Pryce, Proc. Royal Soc. (London) A63, 25 (1950)

14. J. Kanamori, Phys. Chem. Solids 10, 87 (1959)

15. J. Ginter, J. Kossut, and L. Swierkowski, Phys. Stat. Sol. (b) 96, 735 (1979)

16. S.J. Nettel, E.J. Johnson and A. Lempicki, J. Appl. Phys. 49, 464 (1978)

17. J. Villain, J. Phys. Chem. Solids 11, 303 (1959)

18. R.M. White and T.H. Geballe, Solid State Physics 35, Ehrenreich, Seitz, and Turnbull Eds., Academic Press, (New York 1979), p. 136

19. R.W. Davies (private communication)

Appendix C. (Preprint)

PHOTOEMISSION DETERMINATION OF THE OCCUPIED d-BAND POSITION FOR $CdCr_2Se_4$ AND $CdCr_2S_4$

W.J. Miniscalco and B.C. McCollum
GTE Laboratories, Inc., Waltham, Massachusetts 02154

and

N.G. Stoffel and G. Margaritondo
Department of Physics, University of Wisconsin,
Madison, Wisconsin 53706

ABSTRACT

Photoemission spectroscopy has been used to investigate the valence band of $CdCr_2Se_4$ and $CdCr_2S_4$. The occupied d-bands for both materials have been found to lie below the top of the valence band. These results are in qualitative agreement with recent band structure calculations and establish the electronic structure of these materials. Implications for the unusual behavior of their transport properties and absorption edge are discussed.

Chromium chalcogenide spinel magnetic semiconductors have attracted great attention because of the interaction between their magnetic and electronic systems. It has become apparent that the dominant role in these processes is played by excitations in the d-bands rather than in the valence and conduction bands. The locations of the d-bands contributed by the stoichiometric Cr, however, have remained controversial. Using synchrotron radiation photoemission, we have examined the valence band density of states and resolved this question for $CdCr_2Se_4$ and $CdCr_2S_4$, the two best known Cr spinels. Our investigation reveals that the filled d-bands lie below the top of the valence band for both of these materials. These results have important implications for theories of the unusual behavior of their absorption edge and transport properties and facilitate the interpretation of the optical and transport data.

$CdCr_2Se_4$ and $CdCr_2S_4$ are ferromagnetic semiconductors which order at 130 K and 84 K, respectively. Interest in these materials stems from the strong interaction between their carriers and spins, typified for $CdCr_2Se_4$ by an absorption edge which shifts to the red with decreasing temperature[1] and unusual transport properties. The effect of magnetic ordering upon the transport properties manifests itself as strong negative magneto-resistance[2,3] as well as resistivity and Seebeck coefficient anomalies[2,4] in the vicinity of the Curie temperature, T_c. Even more interesting is the converse effect in which variations in carrier concentration produce changes in the ordering temperature. This has been observed for equilibrium carrier concentrations controlled by doping in $HgCr_2Se_4$[5] and $CdCr_2Se_4$.[6] Moreover, dynamic effects produced by optical illumination have been reported for $CdCr_2Se_4$.[7] A feature common to all these manifestations of carrier-spin coupling in chromium chalcogenide spinels is that they are only significant for n-type material.

Attempts to explain these effects have been handicapped by the poor understanding of the electronic structure of these materials which has persisted despite a multitude of optical investigations. There has been no general agreement on the assignment of the optical transitions found, and the observation of luminescence at an energy significantly greater than that of the absorption edge[8] has further complicated matters. This situation has improved somewhat with the recent publication of band structure calculations performed for $CdCr_2Se_4$ and $CdCr_2S_4$ using extended Hückel[9] and discrete variational $X\alpha$ (DV-$X\alpha$)[10] methods. The octahedral symmetry of the Cr site splits the free ion d-levels into a three-fold orbitally degenerate t_{2g} lower state and a two-fold orbitally degenerate e_g upper state. Intra-Cr exchange introduced a large splitting between the spin components of these states and

pushes the levels with antiparallel spin into the conduction band.[9,10] Although significant mixing with anion valence states occurs,[10] for simplicity we shall retain the t_{2g} and e_g labels for the d-bands.

Additional clarification of the electronic structure has been provided by the photoluminescence investigation of Yao et al.[11] which explained the large discrepancy in energy between the absorption edge and the emission by identifying the fundamental gap (valence band to conduction band) for $CdCr_2Se_4$. They found that luminescence results from transitions at the fundamental gap while d-bands in this gap are responsible for the absorption edge at lower energy.[11] Although the band structure calculations[9,10] are in qualitative agreement with the photoluminescence and other optical measurements, until now there has been no unambiguous experimental determination of which d-bands (the filled t_{2g}, unfilled e_g, or both) occupy the fundamental gap and control the transport properties and the position of the absorption edge.

The experiments were performed using synchrotron radiation from the 240 MeV storage ring at the Synchrotron Radiation Center of the University of Wisconsin-Madison. Details of the apparatus and techniques used can be found in Ref. 12. The $CdCr_2Se_4$ crystals were grown by the flux method[13] and the $CdCr_2S_4$ samples were grown by vapor transport.[14] The lattice parameters were verified by x-ray powder patterns and spectrochemical analysis revealed only trace impurities. As an additional test samples were subjected to scanning electron microprobe analysis and no variations in composition were found across the faces. Clean surfaces were obtained by grinding <u>in situ</u> under ultra-high vacuum and photoemission spectra from before and after grinding were compared to insure that no surface contamination remained. All measurements were made at room temperature.

Figures 1 and 2 show the photoelectron kinetic energy distribution curves (EDC's) for $CdCr_2Se_4$ and $CdCr_2S_4$, respectively. The positions of the peaks are independent of photon energy for $CdCr_2S_4$ and, with the exception of two features, for $CdCr_2Se_4$ as well. This indicates that the spectra are true representations of the valence band density of states. The large peak at the left in both Figures 1 and 2 is the Cd 4d core level which has been observed at roughly the same position for the non-magnetic semiconductors $CdIn_2Se_4$[15] and $CdIn_2S_4$.[16] For both Cr spinels there is a feature just below the top of the valence band which is enhanced relative to the rest of the valence band with increasing photon energy. This is the expected behavior of the matrix element for d to f transitions.[17] Indeed, for the related non-magnetic semiconductors $CdIn_2Se_4$ and $CdIn_2S_4$ which contain no d-bands, the upper valence band states exhibit just the opposite dependence on photon energy.[15,16] Accordingly, we identify these features as the occupied t_{2g} d-bands. The DV-Xα calculation also predicts approximately

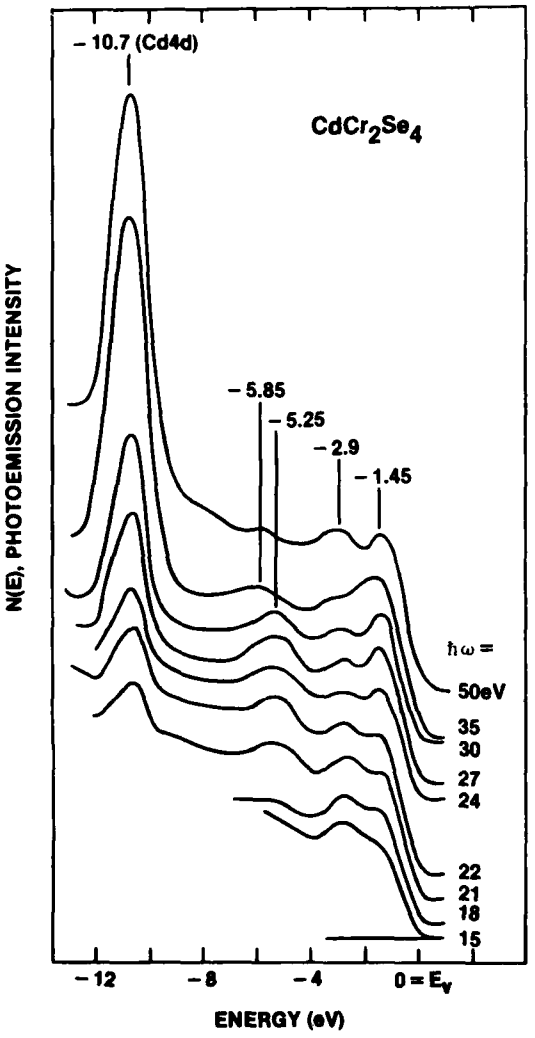

Fig. 1. $CdCr_2Se_4$ EDC's shown for photon energies ranging from 15 eV to 50 eV. The zero of energy has been assigned to the top of the valence band, E_v. The filled t_{2g} d-band corresponds to the peak at -1.45 eV which is enhanced with increasing photon energy.

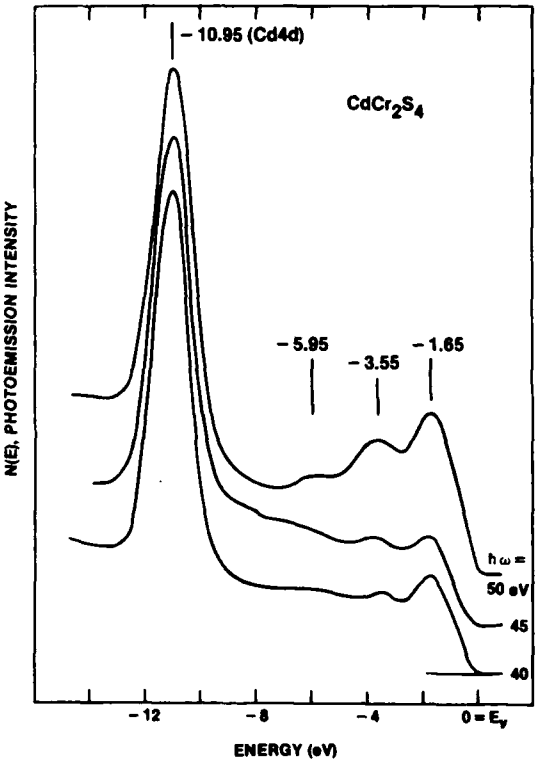

Fig. 2. $CdCr_2S_4$ EDC's shown for photon energies range from 40 eV to 50 eV. The zero of energy has been assigned to the top of the valence band, E_v. The filled t_{2g} d-band correspond to the peak at -1.65 eV which is enhanced with increasing photon energy.

this position for the parallel spin t_{2g} states and we conclude that the correct electronic structure for these two materials is that illustrated in Figure 3. For $CdCr_2Se_4$ the occupied d-bands are located 1.45 eV below the top of the valence band and for $CdCr_2S_4$ they are 1.65 eV below the top of the valence band.

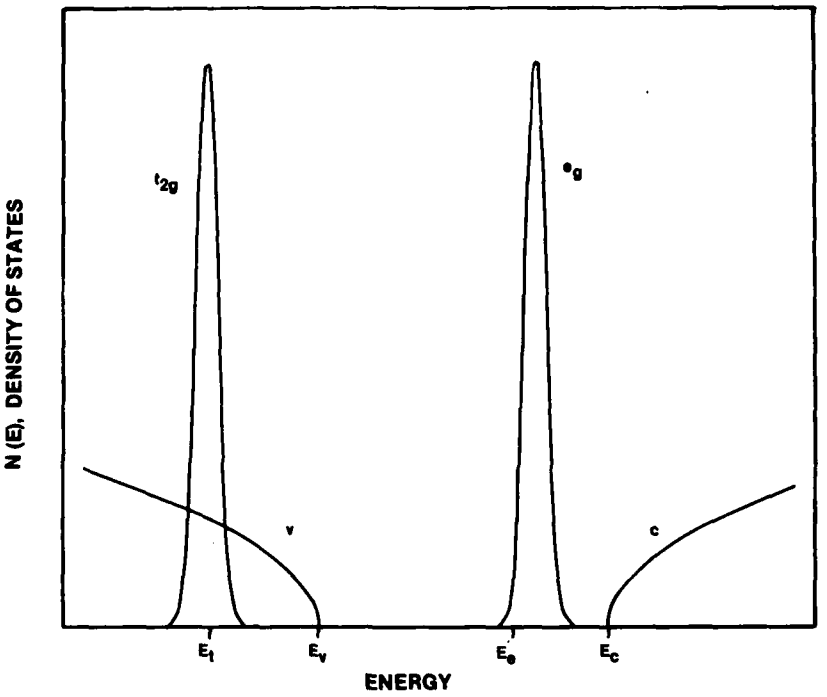

Fig. 3. The electronic structure of $CdCr_2Se_4$ and $CdCr_2S_4$ based upon photoemission and photoluminescence data. Only the parallel spin t_{2g} and e_g d-bands are shown; the antiparallel components are in the conduction band. The fundamental gap is E_c-E_v. For $CdCr_2Se_4$, E_v-E_t is 1.45 eV and for $CdCr_2S_4$ it is 1.65 eV. The absorption edge is given by E_e'-E_v.

The extended Hückel calculation[9] gives the same size fundamental gap for $CdCr_2Se_4$ as the photoluminescence measurements.[8,11] However, it places both the parallel spin t_{2g} and e_g bands in the fundamental gap for these materials in contradiction with the photoemission results. The ab initio DV-Xα calculation[10] is more accurate and for $CdCr_2Se_4$ it places the occupied t_{2g} band just below the top of the valence band in agreement with our measurements. For $CdCr_2S_4$, however, the calculation disagrees with our photoemission data and shows the filled d-band extending above the top of the valence band. These comparisons are valid even though the measurements were done for the paramagnetic state while the DV-Xα calculations are for the ferromagnetic state. This is because the spin-splittings for the valence band (~.1 eV)[10] are negligible on the energy scale of interest. Moreover, intra-atomic exchange (~3 eV) largely determines the spin-splittings of the d-bands so the positions of these differ little between the paramagnetic and ferromagnetic state.

Our results and the DV-Xα calculation for $CdCr_2Se_4$ are consistent with the available transport measurements. Lehmann and Harbeke[18] reported electron mobilities two orders of magnitude smaller than hole mobilities for $CdCr_2Se_4$. This has been interpreted as indicating hole conductivity takes place in wide bands while electron conductivity occurs in narrow bands. This is the behavior expected for the electronic structure of Figure 3 which requires that holes be in the valence band while electrons are in the relatively narrow e_g band. Although similar mobility measurements are lacking for $CdCr_2S_4$, we expect identical behavior since our data indicate that its electronic structure is qualitatively the same. In the absence of small polaron formation this electronic structure requires that donor levels lie below the parallel spin e_g band for the material to be semiconducting. Shallow donor levels associated with the conduction edge (E_c in Figure 3) would result in metallic conductivity for n-type material rather than the activated conductivity observed above T_c.[2] For the present this question remains open since the paramagnetic state is one of great disorder for the e_g band and facilitates small polaron formation.[19]

The location of the filled d-bands below the top of the valence band has important implications for the carrier-spin coupling. It is now possible to conclude that only transitions from the top of the valence band to the empty e_g band contribute to the absorption edge. The latter corresponds to the energy difference $E_e' - E_v$ in Figure 3. Since the fundamental gap for $CdCr_2Se_4$ ($E_c - E_v$ in Figure 3) increases with decreasing temperature as is typical for non-magnetic semiconductors,[11] the red-shifting absorption edge results from a lowering of the e_g band extremum E_e' with decreasing temperature. This can occur as either a rigid shift or broadening of the e_g band as a function of magnetic ordering. In addition, the existence of

anomalies in the transport properties near T_c only for n-type material indicates that these effects as well are associated with the e_g band. The resistivity peak near T_c can be explained by an increase in electron mobility below T_c if the e_g band broadens with increasing magnetic ordering.[20] However, Hall measurements indicate that the reduction in resistivity is produced by a large increase in electron concentration.[4] Although these questions have yet to be resolved, the verification of the electronic structure in Figure 3 for $CdCr_2Se_4$ and $CrCr_2S_4$ demonstrates why similar effects of magnetic ordering are not observed for hole conduction since this occurs in the valence band. It also requires that any realistic theories of these effects take into account that the parallel spin e_g band is responsible for both electron transport and the red shifting absorption edge.

The crystals were grown by D. Guenther. We wish to thank the staff members of the University of Wisconsin Synchrotron Radiation Center for their hospitality and invaluable assistance. Acknowledgement is also due A. Lempicki, R.W. Davies, and E.J. Johnson for much helpful discussion. Work at GTE Laboratories was supported in part by the Air Force Office of Scientific Research under Contract No. F49620-79-C-0182. Work at the University of Wisconsin was supported in part by NSF under Grant No. DMR 78-22205. The Synchrotron Radiation Center is supported by NSF Grant No. DMR 77-21888.

REFERENCES

1. G. Busch, B. Magyar, P. Wachter, Physics Lett. 23, 438 (1966); G. Harbeke, H. Pinch, Phys. Rev. Lett. 17, 1090 (1966).

2. H.W. Lehmann, Phys. Rev. 163, 488 (1967).

3. C. Haas, A.M.J.G. van Run, P.F. Bongers, W. Alber, Solid State Commun. 5, 657 (1967).

4. A. Amith, G.L. Gunsalus, J. Appl. Phys. 40, 1020 (1969).

5. A. Selmi, P. Gibart, L. Goldstein, J. Magn. Magn. Materials 15, 1285 (1980).

6. A.A. Minakov, G.L. Vinogradova, K.M. Golant, V.H. Makhotkin, V.G. Veselago, Sov. Phys. Solid State 19, 1214 (1977).

7. W. Lems, P.J. Bongers, U. Enz, Phys. Rev. Lett. 21, 1643 (1968); S.G. Rudov, V.G. Veselago, Sov. Phys. Solid State 21, 1875 (1979).

8. V.G. Veselago, I.A. Damaskin, S.L. Pyshkin, S.I. Radautsan, V.E. Tézlévan, JETP Lett. 20, 149 (1974).

9. T. Kambara, T. Oguchi, K.I. Gondaira, J. Phys. C 13, 1493 (1980).

10. T. Oguchi, T. Kambara, K.I. Gondaira, Phys. Rev. B 22, 872 (1980).

11. S.S. Yao, F. Pellegrino, R.R. Alfano, W.J. Miniscalco, A. Lempicki, Phys. Rev. Lett. 46, 558 (1981).

12. G. Margaritondo, J.H. Weaver, N.G. Stoffel, J. Phys. E 12, 662 (1979).

13. G.H. Larsen, A.W. Sleight, Phys. Lett. 28A, 203 (1968).

14. H.L. Pinch, S.B. Berger, J. Phys. Chem. Solids 29, 2091 (1968).

15. P. Picco, I. Abbati, L. Braicovich, F. Cerrina, F. Levy, G. Margaritondo, Physics Lett. 65A, 447 (1978).

16. F. Cerrina, C. Quaresima, I. Abbati, L. Braicovich, P. Picco, G. Margaritondo, Solid State Commun. 33, 429 (1980).

17. U. Fano, J.W. Cooper, Rev. Mod. Phys. 40, 441 (1968).

18. H.W. Lehmann, G. Harbeke, J. Appl. Phys. 38, 946 (1967).

19. D. Emin, in Electrical and Structural Properties of Amorphous Semiconductors, edited by P.G. Le Comber and J. Mort (Academic, New York, 1973), p. 261.

20. M.D. Coutinho-Filho, I. Balberg, J. Appl. Phys. 50, 1920 (1979).

Appendix D.

PHOTOLUMINESCENT SPECTRA AND KINETICS OF $CdCr_2Se_4$ AND $CdCr_2S_4$

W.J. Miniscalco and A. Lempicki
GTE Laboratories, Inc., 40 Sylvan Road, Waltham, MA 02254
USA

and

S.S. Yao, F. Pellegrino, R.R. Alfano
Physics Dept., City College of NY, New York, NY 10031
USA

PHOTOLUMINESCENT SPECTRA AND KINETICS OF $CdCr_2Se_4$ AND $CdCr_2S_4$

W. J. Miniscalco and A. Lempicki
GTE Laboratories, Inc., 40 Sylvan Road, Waltham, MA 02254
USA

and

S. S. Yao, F. Pellegrino, R. R. Alfano
Physics Dept., City College of NY, New York, NY 10031
USA

Photoluminescence at the fundamental gap has been used to clarify the electronic structure of the ferromagnetic semiconductors $CdCr_2Se_4$ and $CdCr_2S_4$. For the latter this is the first report of band gap emission. For $CdCr_2Se_4$ luminescence spectra and decay have been measured and analyzed as a function of temperature and the quantum efficiency has been determined at 77 K. Implications of these results for recent band structure calculations and photoemission measurements are considered.

Chromium chalcogenide spinel magnetic semiconductors have attracted considerable interest because of the interaction between their electronic and magnetic systems. Despite the large amount of effort directed toward these materials, their electronic structure has remained controversial. We report photoluminescence measurements which identify the fundamental gap for the two most extensively studied Cr spinels, $CdCr_2Se_4$ and $CdCr_2S_4$. In combination with a recent photoemission investigation,[1] these measurements determine the qualitative electronic structure of these two compounds.

$CdCr_2Se_4$ and $CdCr_2S_4$ are ferromagnetic semiconductors which order at 130 K and 84 K, respectively. These materials have attracted special attention because of the strong interaction between their carriers and spins, typified for $CdCr_2Se_4$ by an absorption edge which shifts to the red with decreasing temperature[2] and unusual transport properties in the vicinity of the Curie temperature.[3] In addition, $CdCr_2Se_4$ displays optically induced permeability changes[4] which may result from magnetization changes.[5] Attempts to explain these effects have been handicapped by the poor understanding of the electronic structure of chromium chalcogenide spinels which has persisted despite extensive study by a wide variety of optical and transport techniques. Photoluminescence was first observed for $CdCr_2Se_4$ by Veselago et al.[6] who attributed it to transitions between crystal field split states of Cr^{3+} (R-line emission). This luminescence is difficult to assign because it lies at higher energy than the absorption edge (1.8 eV vs. 1.2 eV at 77 K).

Recent photoluminescence measurements by Yao et al.[7] have reinterpreted this as band gap emission. Using photoconductivity, Larsen and Wittekoek[8] found a band gap of 2.5 eV for $CdCr_2S_4$ but did not observe luminescence at this energy. New insight into the electronic structure of these materials has been added by band structure calculations performed using the extended Huckel[9] and discrete variational Xα[10] (DV-Xα) methods.

The octahedral symmetry of the Cr site splits the free ion d-levels into a three-fold orbitally degenerate t_{2g} lower state and a two-fold orbitally degenerate e_g upper state. Intra-Cr exchange should introduce a large splitting between the spin components of these states. With regard to the electronic structure, the most important questions concern the locations of these d-bands with respect to the p-like valence band and s-like conduction band. To experimentally clarify the electronic structure of $CdCr_2S_4$ we have measured quantum efficiency at 77 K as well as luminescence decay, line shape, and line position as a function of temperature. In addition, we report the first observations of fundamental gap luminescence for $CdCr_2S_4$.

The experiments were performed with use of cw, nanosecond-pulse, and picosecond-pulse excitation. For line shape analysis, low power (≤10 mW) cw excitation was provided by the 488 nm line of an argon ion laser. A nitrogen-laser-pumped dye laser system was used to excite $CdCr_2S_4$. With both these excitation sources the emission was analyzed with spectrometers and detected with conventional photomultipliers. In the decay measurements, picosecond excitation was provided by a frequency doubled (530 nm), mode-locked Nd:glass laser (pulse width ≈ 6 ps) with detection by a 10-ps-resolution streak camera used in combination with bandpass filters. Single crystal samples typically 1 mm on a side were mounted in optical cryostats and cooled by flowing N_2 gas.

The $CdCr_2Se_4$ crystals were grown by the flux method[11] and the $CdCr_2S_4$ samples were grown by vapor transport.[12]. The lattice parameters were verified by X-ray powder patterns and spectrochemical analysis revealed only trace impurities. As an additional test, samples were subjected to scanning electron microprobe analysis and no variations in composition were found across the faces.

The luminescence decay measurements for $CdCr_2Se_4$ revealed a lifetime of 25 ps at 77 K which decreases to a few picoseconds at 250 K. These very short lifetimes indicate that the relaxation of the excited state is dominated by nonradiative decay or transitions to intermediate states. This conclusion is confirmed by quantum efficiency measurements made by comparing the 1.8 eV emission to that of Rhodamine 6G. An efficiency of 10^{-4} was found in this way. This value is probably an underestimate because of the strong self-absorption at this energy. Combining the decay and quantum efficiency measurements produces a lower limit for the radiative transition rate of $4X10^6$

sec^{-1}. This is too large a value for a parity forbidden transition and precludes the possibility that the transition is between crystal field $3d^3$ states of Cr for which the transition rates are at least three orders of magnitude smaller.

The decay measurements are also useful in explaining why the absorption edge is at lower energy than the luminescence in these materials. For compound semiconductors, one expects the band states to be strongly coupled to polar optical modes[13] and relax via intraband, phonon-emitting processes on a subpicosecond time scale.[14] The 25 ps decay time at 77 K requires a gap or bottleneck between the levels involved in the radiative transition and the lower-lying ones involved in the 1.2 eV absorption edge. The simplest electronic structure consistent with this requirement has a 1.8 eV fundamental gap, E_g, with d-bands in this gap responsible for the absorption edge. From absorption and photoluminescence data alone it is not possible to determine whether the d-bands in the gap are the filled t_{2g}, unfilled e_g, or both.

As a further test of the nature of the $CdCr_2Se_4$ emission, the temperature dependence of the peak was measured. This shifts to the blue with decreasing temperature in contrast to the absorption edge which shifts to the red. For interband transitions the luminescence peak lies from $\frac{1}{2}kT$ to $2kT$ higher in energy than E_g depending on whether the transition is direct or indirect.[15] Using this relationship between E_g and the luminescence peak yields a band gap with the quadratic temperature dependence typical of non-magnetic semiconductors.[16] The line shape analysis also indicates that the emission involves band states. Under moderate excitation conditions free carriers are described by a Maxwell-Boltzmann distribution.[13] The Boltzmann factor will accordingly appear in the line shape of the recombination radiation. By fitting exponentials to the high energy edge of lines measured at low excitation levels, we deduced carrier temperatures which fell within experimental uncertainty of the sample temperatures over the range 80 to 200 K. The carrier temperature is expected to deviate little from that of the lattice at these high sample temperatures and low excitation levels.

In contrast to the single line observed at 1.8 eV for $CrCr_2Se_4$, the fundamental gap photoluminescence of $CdCr_2S_4$ consists of several rather weak lines extending from 2.5 eV down to 2.3 eV. These were observed under pulsed excitation at 450 nm and a temperature of 77 K. Although lifetime and temperature-dependence measurements are not yet available, it is possible to conclude that the fundamental gap of $CdCr_2S_4$ is $\approx$2.5 eV. This is in agreement with the value obtained by photoconductivity.[8] The emission lines at lower energy are likely due to traps.

Recent photoemission measurements by Miniscalco et al.[1] have determined that the occupied t_{2g} d-bands lie below the top of the valence band for both $CrCr_2Se_4$ and $CdCr_2S_4$. By combining the photoemission and

photoluminescence results it is possible to ascertain that it is only the unfilled e_g band which occupies the fundamental gap. The experimentally determined electronic structure qualitatively supports the band structure calculations. The extended Huckel calculation gives 1.7 eV for the band gap of $CdCr_2Se_4$ and the 2.5 eV for $CdCr_2S_4$.[9] The corresponding values from photoluminescence are 1.8 eV and 2.5 eV. However, the Huckel calculation places both the t_{2g} and the e_g bands in the fundamental gap in contradiction with the photoemission measurements. The DV-Xα calculation gives larger values for E_g than photoluminescence, 2.3 eV for $CdCr_2Se_4$ and 2.6 eV for $CdCr_2S_4$.[10] For $CdCr_2Se_4$ it places the t_{2g} band below the top of the valence band in agreement with the photoemission results. For $CdCr_2S_4$, however it disagrees and shows the t_{2g} band extending above the top of the valence band. These discrepancies remain to be resolved.

The crystals were grown by B. C. McCollum, J. Kafalas, and D. Guenther. We wish to acknowledge much helpful discussion with T. Kambara, E. J. Johnson, S. J. Nettel, and R. W. Davies. This work was supported in part at GTE Laboratories, Inc. by AFOSR contract No. F49620-79-C-0182 and at The City College of New York by grant No. AFOSR-80-0079.

[1] W.J. Miniscalco, B.C. McCollum, N.G. Stoffel, and G. Margaritondo, to be published.

[2] B. Busch, B. Magyar, and P. Watchter, Physics Lett. 23 (1966) 438; G. Harbeke and H. Pinch, Phys. Rev. Lett. 17 (1966) 1090.

[3] H.W. Lehmann, Phys. Rev. 163 (1967) 488; C. Haas, A.M.J.G. van Run, P.F. Bongers and W. Alber, Solid State Commun. 5 (1967) 657; A. Amith and G.L. Gunsalus, J. Appl. Phys. 40 (1969) 1020.

[4] W. Lems, P.J. Rijnierse, P.F. Bongers, and U. Enz, Phys. Rev. Lett. 21 (1968) 1643.

[5] N.M. Salanskii and N.A. Drokin, Fiz. Tverd. Tela (Leningrad) 17 (1975) 331 [Sov. Phys. Solid State 17 (1975) 205].

[6] V.G. Veselago, I.A. Damaskin, S.L. Pyshkin, S.I. Radautsan, and V.E. Tezlevan, Pis'ma Zh. Eksp. Teor. Fiz. 20 (1974) 335 [JETP Lett. 20 (1974) 149]; V.G. Veselago, Colloq. Int. C.N.R.S. 242 (1974) 295.

[7] S.S. Yao, F. Pellegrino, R.R. Alfano, W.J. Miniscalco, and A. Lempicki, Phys. Rev. Lett. 46 (1981) 558.

[8] P.K. Larsen and S. Wittekoek, Phys. Rev. Lett. 29 (1972)

1597.

[9] T. Kambara, T. Oguchi, and K.I. Gondaira, J. Phys. C 13 (1980) 1493.

[10] T. Oguchi, T. Kambara, and K.I. Gondaira, Phys. Rev. B 22 (1980) 872.

[11] G.H. Larsen and A.W. Sleight, Phys. Lett. 28A (1968) 203.

[12] H.L. Pinch and S.B. Berger, J. Phys. Chem. Solids 29 (1968) 2091.

[13] J. Shah, Phys. Rev. B 9 (1974) 562.

[14] C.V. Shank, R.L. Fork, R.F. Leheny, and J. Shah, Phys. Rev. Lett. 42 (1979) 112.

[15] R.J. Elliott, Phys. Rev. 108 (1957) 1384.

[16] G.D. Mahan, J. Phys. Chem. Solids 26 (1965) 751.

APPENDIX E

MATRIX ELEMENTS FOR THE IRREDUCIBLE REPRESENTATIONS OF THE DOUBLE GROUP OF O_h^7 AT SIX HIGH SYMMETRY POINTS

TABLE E-1

Γ- POINT (ZONE CENTER)

The necessary matrix elements at the Γ- point, in particular, the matrix elements for the extra representations $\Gamma_6^{\pm}$, $\Gamma_7^{\pm}$, $\Gamma_8^{\pm}$ are listed in Tables A9-8 and A9-11 of Slater's book.[42] It should be noted that Slater's $\Gamma_8^{\pm}$ representations are not unitary. This can be remedied using a procedure described by Tinkham.[43]

Note: The notation for the various symmetry operations, R_1, R_2, R_3....is identical to that which appears on page 28 of Slater's book.[42]

TABLE E-2

THE EXTRA REPRESENTATION AT THE X-POINT

$$X_5(R_1) = \begin{pmatrix} 1 & 0 & 0 & 0 \\ 0 & 1 & 0 & 0 \\ 0 & 0 & 1 & 0 \\ 0 & 0 & 0 & 1 \end{pmatrix} \qquad X_5(R_2) = \begin{pmatrix} 0 & i & 0 & 0 \\ i & 0 & 0 & 0 \\ 0 & 0 & 0 & i \\ 0 & 0 & i & 0 \end{pmatrix}$$

$$X_5(R_3) = \begin{pmatrix} 0 & 1 & 0 & 0 \\ -1 & 0 & 0 & 0 \\ 0 & 0 & 0 & -1 \\ 0 & 0 & 1 & 0 \end{pmatrix} \qquad X_5(R_4) = \begin{pmatrix} i & 0 & 0 & 0 \\ 0 & -i & 0 & 0 \\ 0 & 0 & -i & 0 \\ 0 & 0 & 0 & i \end{pmatrix}$$

$$X_5(R_{13}) = \frac{1}{\sqrt{2}} \begin{pmatrix} 1 & i & 0 & 0 \\ i & 1 & 0 & 0 \\ 0 & 0 & -1 & -i \\ 0 & 0 & -i & -1 \end{pmatrix} \qquad X_5(R_{14}) = \frac{1}{\sqrt{2}} \begin{pmatrix} 1 & -i & 0 & 0 \\ -i & 1 & 0 & 0 \\ 0 & 0 & -1 & i \\ 0 & 0 & i & -1 \end{pmatrix}$$

$$X_5(R_{19}) = \frac{1}{\sqrt{2}} \begin{pmatrix} -i & 1 & 0 & 0 \\ -1 & i & 0 & 0 \\ 0 & 0 & -i & 1 \\ 0 & 0 & -1 & i \end{pmatrix} \qquad X_5(R_{20}) = \frac{1}{\sqrt{2}} \begin{pmatrix} -i & -1 & 0 & 0 \\ 1 & i & 0 & 0 \\ 0 & 0 & -i & -1 \\ 0 & 0 & 1 & i \end{pmatrix}$$

TABLE E-2 (Cont.)

$$X_5(R_1') = \begin{pmatrix} 0 & 0 & 1 & 0 \\ 0 & 0 & 0 & 1 \\ 1 & 0 & 0 & 0 \\ 0 & 1 & 0 & 0 \end{pmatrix} \qquad X_5(R_2') = \begin{pmatrix} 0 & 0 & 0 & i \\ 0 & 0 & i & 0 \\ 0 & i & 0 & 0 \\ i & 0 & 0 & 0 \end{pmatrix}$$

$$X_5(R_3') = \begin{pmatrix} 0 & 0 & 0 & 1 \\ 0 & 0 & -1 & 0 \\ 0 & -1 & 0 & 0 \\ 1 & 0 & 0 & 0 \end{pmatrix} \qquad X_5(R_4') = \begin{pmatrix} 0 & 0 & i & 0 \\ 0 & 0 & 0 & -i \\ -i & 0 & 0 & 0 \\ 0 & i & 0 & 0 \end{pmatrix}$$

$$X_5(R_{13}') = \frac{1}{\sqrt{2}} \begin{pmatrix} 0 & 0 & 1 & i \\ 0 & 0 & i & 1 \\ -1 & -i & 0 & 0 \\ -i & -1 & 0 & 0 \end{pmatrix} \qquad X_5(R_{14}') = \frac{1}{\sqrt{2}} \begin{pmatrix} 0 & 0 & 1 & -i \\ 0 & 0 & -i & 1 \\ -1 & i & 0 & 0 \\ i & -1 & 0 & 0 \end{pmatrix}$$

$$X_5(R_{19}') = \frac{1}{\sqrt{2}} \begin{pmatrix} 0 & 0 & -i & 1 \\ 0 & 0 & -1 & i \\ -i & 1 & 0 & 0 \\ -1 & i & 0 & 0 \end{pmatrix} \qquad X_5(R_{20}') = \frac{1}{\sqrt{2}} \begin{pmatrix} 0 & 0 & -i & -1 \\ 0 & 0 & 1 & i \\ -i & 1 & 0 & 0 \\ 1 & i & 0 & 0 \end{pmatrix}$$

TABLE E-3

THE EXTRA REPRESENTATIONS AT THE L-POINT

(a) The One-Dimensional Extra Representations at the L-Point

	R_1	R_5	R_9	R_{19}	R_{21}	R_{23}	R'_1	R'_5	R'_9	R'_{19}	R'_{21}	R'_{23}
L_4^+	1	-1	-1	i	i	i	1	-1	-1	i	i	i
L_4^-	1	-1	-1	-i	-i	-i	-1	1	1	i	i	i
L_5^+	1	-1	-1	-i	-i	-i	1	-1	-1	-i	-i	-i
L_5^-	1	-1	-1	i	i	i	-1	1	1	-i	-i	-i

(b) The Two-Dimensional Extra Representations at the L-Point

$$L\,\tfrac{+}{6}\,(R_1) = \begin{pmatrix} 1 & 0 \\ 0 & 1 \end{pmatrix} \qquad L\,\tfrac{+}{6}\,(R_5) = \frac{1}{2}\begin{pmatrix} 1-i & -1-i \\ 1-i & 1+i \end{pmatrix}$$

$$L\,\tfrac{+}{6}\,(R_9) = \frac{1}{\sqrt{2}}\begin{pmatrix} 1+i & 1+i \\ -1+i & 1-i \end{pmatrix} \qquad L\,\tfrac{+}{6}\,(R'_{19}) = \frac{1}{\sqrt{2}}\begin{pmatrix} -i & 1 \\ -1 & i \end{pmatrix}$$

$$L\,\tfrac{+}{6}\,(R'_{21}) = \frac{1}{\sqrt{2}}\begin{pmatrix} i & -i \\ -i & -i \end{pmatrix} \qquad L\,\tfrac{+}{6}\,(R'_{23}) = \begin{pmatrix} 0 & \frac{-1+i}{\sqrt{2}} \\ \frac{1+i}{\sqrt{2}} & 0 \end{pmatrix}$$

The matrices for the remaining 6 improper rotations, R'_1, R'_5, R'_9, R_{19}, R_{21}, R_{23}, may be obtained using the relation

$$L\,\tfrac{+}{6}\,(R'_i) = \pm\, L\,\tfrac{+}{6}\,(R_i).$$

TABLE E-4

THE EXTRA REPRESENTATIONS AT THE W-POINT

(a) The One-Dimensional Extra Representations at the W-Point

	R_1	R_3	R_{15}	R_{16}	R'_2	R'_1	R'_{21}	R'_{22}
W_3	1	i	$\frac{1+i}{\sqrt{2}}$	$\frac{1-i}{\sqrt{2}}$	$\frac{1-i}{\sqrt{2}}$	$\frac{1+i}{\sqrt{2}}$	i	-1
W_4	1	i	$\frac{-1-i}{\sqrt{2}}$	$\frac{-1+i}{\sqrt{2}}$	$\frac{-1+i}{\sqrt{2}}$	$\frac{-1-i}{\sqrt{2}}$	i	-1
W_5	1	i	$\frac{1+i}{\sqrt{2}}$	$\frac{1-i}{\sqrt{2}}$	$\frac{-1+i}{\sqrt{2}}$	$\frac{-1-i}{\sqrt{2}}$	-i	1
W_6	1	i	$\frac{-1-i}{\sqrt{2}}$	$\frac{-1+i}{\sqrt{2}}$	$\frac{1-i}{\sqrt{2}}$	$\frac{1+i}{\sqrt{2}}$	-i	1

(b) The Two-Dimensional Extra Representation at the W-Point

$$W_7\ (R_1) = \begin{pmatrix} 1 & 0 \\ 0 & 1 \end{pmatrix} \qquad W_7\ (R_3) = \begin{pmatrix} -i & 0 \\ 0 & -i \end{pmatrix}$$

$$W_7\ (R_{15}) = \frac{1+i}{\sqrt{2}} \begin{pmatrix} 0 & 1 \\ -1 & 0 \end{pmatrix} \qquad W_7\ (R_{16}) = \frac{1-i}{\sqrt{2}} \begin{pmatrix} 0 & -1 \\ 1 & 0 \end{pmatrix}$$

$$W_7\ (R'_2) = \frac{1-i}{\sqrt{2}} \begin{pmatrix} 1 & 0 \\ 0 & -1 \end{pmatrix} \qquad W_7\ (R'_4) = \frac{1+i}{\sqrt{2}} \begin{pmatrix} -1 & 0 \\ 1 & 0 \end{pmatrix}$$

$$W_7\ (R'_{21}) = \begin{pmatrix} 0 & i \\ i & 0 \end{pmatrix} \qquad W_7\ ('_{22}) = \begin{pmatrix} 0 & 1 \\ 1 & 0 \end{pmatrix}$$

TABLE E-5

THE EXTRA REPRESENTATIONS AT THE Δ- POINT

With $\vec{k}_x = k_x \hat{x}$ the reduced wave vector at the Δ- point, and with $\vec{\tau} = \frac{a}{4}(1,1,1)$, we define a parameter $\alpha \equiv e^{i \vec{k}_x \cdot \vec{\tau}} = e^{i k_x a/4}$.

The matrices are then as follows:

$$\Delta_6(R_1) = \Delta_7(R_1) = \begin{pmatrix} 1 & 0 \\ 0 & 1 \end{pmatrix}$$

$$\Delta_6(R_2) = \Delta_7(R_2) = \begin{pmatrix} 0 & i \\ i & 0 \end{pmatrix}$$

$$\Delta_6(R_{19}) = -\Delta_7(R_{19}) = \frac{1}{\sqrt{2}} \begin{pmatrix} -i & 1 \\ -1 & i \end{pmatrix}$$

$$\Delta_6(R_{20}) = -\Delta_7(R_{20}) = \frac{1}{\sqrt{2}} \begin{pmatrix} -i & -i \\ 1 & i \end{pmatrix}$$

$$\Delta_6(R_3') = \Delta_7(R_3') = \alpha \begin{pmatrix} 0 & 1 \\ -1 & 0 \end{pmatrix}$$

$$\Delta_6(R_4') = \Delta_7(R_4') = \alpha \begin{pmatrix} i & 0 \\ 0 & -i \end{pmatrix}$$

$$\Delta_6(R_{13}') = -\Delta_7(R_{13}') = \frac{\alpha}{\sqrt{2}} \begin{pmatrix} 1 & i \\ i & 1 \end{pmatrix}$$

$$\Delta_6(R_{14}') = -\Delta_7(R_{14}') = \frac{\alpha}{\sqrt{2}} \begin{pmatrix} 1 & -i \\ -i & 1 \end{pmatrix}$$

TABLE E-6

THE EXTRA REPRESENTATIONS AT THE Λ - POINT

(a) One Dimensional Extra Representations at the Λ - Point

	R_1	R_5	R_9	R_{19}	R_{21}	R_{23}
Λ_4	1	-1	-1	i	i	i
Λ_5	1	-1	-1	-i	-i	-i

(b) The Two-Dimensional Extra Representation at the Λ - Point

$$\Lambda_6\ (R_1) = \begin{pmatrix} 1 & 0 \\ 0 & 1 \end{pmatrix} \qquad \Lambda_6\ (R_5) = \frac{1}{2} \begin{pmatrix} 1-i & -1-i \\ 1-i & 1+i \end{pmatrix}$$

$$\Lambda_6\ (R_9) = \frac{1}{2} \begin{pmatrix} 1+i & 1+i \\ -1+i & 1-i \end{pmatrix} \qquad \Lambda_6\ (R_{19}) = \frac{1}{\sqrt{2}} \begin{pmatrix} -i & 1 \\ -1 & i \end{pmatrix}$$

$$\Lambda_6\ (R_{21}) = \frac{1}{\sqrt{2}} \begin{pmatrix} i-i \\ -i-i \end{pmatrix} \qquad \Lambda_6\ (R_{23}) = \frac{1}{\sqrt{2}} \begin{pmatrix} 0 & -1+i \\ 1+i & 0 \end{pmatrix}$$


DAI
ILM